JGR Atmospheres

RESEARCH ARTICLE
10.1029/2025JD043677

Wintertime Abundance and Sources of Key Trace Gas and Particle Species in Fairbanks, Alaska

Damien T. Ketcherside[1], Robert J. Yokelson[1], Vanessa Selimovic[1,2], Ellis S. Robinson[3], Meeta Cesler-Maloney[4], Andrew L. Holen[5], Judy Wu[5], Brice Temime-Roussel[6], Amna Ijaz[6,7], Jonas Kuhn[8], Allison Moon[9], Gianluca Pappaccogli[10], Karolina Cysneiros de Carvalho[11], Stefano Decesari[10], Becky Alexander[9], Brent J. Williams[11,12], Barbara D'Anna[6], Jochen Stutz[8], Kerri A. Pratt[5], Peter F. DeCarlo[3], Jingqui Mao[4], William R. Simpson[4], Philip K. Hopke[13,14], and Lu Hu[1]

[1]Department of Chemistry and Biochemistry, University of Montana, Missoula, MT, USA, [2]Now at University of Michigan, Department of Chemistry, Ann Arbor, MI, USA, [3]Department of Environmental Health and Engineering, Johns Hopkins University, Baltimore, MD, USA, [4]Geophysical Institute and Department of Chemistry and Biochemistry, University of Alaska Fairbanks, Fairbanks, AK, USA, [5]Department of Chemistry, University of Michigan, Ann Arbor, MI, USA, [6]CNRS, LCE, Aix Marseille Univ, Marseille, France, [7]Now at Atmospheric, Climate, & Earth Sciences Division, Pacific Northwest National Laboratory, Richland, WA, USA, [8]UCLA Atmospheric & Oceanic Sciences, Los Angeles, CA, USA, [9]Department of Atmospheric and Climate Science, University of Washington, Seattle, WA, USA, [10]Institute of Atmospheric Sciences and Climate (ISAC) of the National Research Council of Italy (CNR), Bologna, Italy, [11]Energy, Environmental, and Chemical Engineering, Washington University in St. Louis, St. Louis, WA, USA, [12]Department of Soil, Water, and Climate, University of Minnesota, St. Paul, MN, USA, [13]School of Medicine and Dentistry, Department of Public Health Sciences, University of Rochester, Rochester, NY, USA, [14]Institute for a Sustainable Environment, Clarkson University, Potsdam, NY, USA

Key Points:

- The wintertime volatile organic compound burden in Fairbanks, AK is higher than more densely populated urban areas, such as New York City
- Traffic is the dominant source of volatile organic compounds in Fairbanks, and heating oil combustion is the main source of particulates
- Secondary chemical processes were observed to have a substantial impact on the budget of many trace gas and particulate species

Supporting Information:

Supporting Information may be found in the online version of this article.

Correspondence to:

R. J. Yokelson,
bob.yokelson@umontana.edu

Citation:

Ketcherside, D. T., Yokelson, R. J., Selimovic, V., Robinson, E. S., Cesler-Maloney, M., Holen, A. L., et al. (2025). Wintertime abundance and sources of key trace gas and particle species in Fairbanks, Alaska. *Journal of Geophysical Research: Atmospheres*, *130*, e2025JD043677. https://doi.org/10.1029/2025JD043677

Received 4 MAR 2025
Accepted 17 JUL 2025

Author Contributions:

Conceptualization: Damien T. Ketcherside, Robert J. Yokelson, Lu Hu
Data curation: Damien T. Ketcherside
Formal analysis: Damien T. Ketcherside, Robert J. Yokelson, Philip K. Hopke
Funding acquisition: Robert J. Yokelson, Gianluca Pappaccogli, Stefano Decesari, Becky Alexander, Brent J. Williams, Barbara D'Anna, Jochen Stutz, Kerri A. Pratt, Peter F. DeCarlo, Jingqui Mao, William R. Simpson, Lu Hu
Investigation: Damien T. Ketcherside, Vanessa Selimovic, Ellis S. Robinson, Meeta Cesler-Maloney, Andrew L. Holen, Judy Wu, Brice Temime-Roussel, Amna Ijaz, Jonas Kuhn, Karolina Cysneiros de Carvalho, Jochen Stutz
Methodology: Damien T. Ketcherside, Robert J. Yokelson, Lu Hu

Abstract We investigated how various sources contributed to observations of over 40 trace gas and particulate species in a typical Fairbanks residential neighborhood during the Alaskan Layered Pollution and Chemical Analysis campaign in January–February 2022. Aromatic volatile organic compounds (VOCs) accounted for ~50% of measured VOCs (molar ratio), while methanol and ethanol accounted for ~34%. The total wintertime VOC burden and contribution from aromatics were much higher than other US urban areas. Based on diel cycles and positive matrix factorization (PMF) analyses, we find traffic was the largest source of NO, CO, black carbon, and aromatic VOCs. Formic and acetic acid, hydroxyacetone, furanoids, and other VOCs were primarily attributed to residential wood combustion (RWC). Formaldehyde was one of several VOCs featuring significant contributions from multiple sources: RWC (~35%), aging (~30%), traffic (~21%), and heating oil combustion (HO, ~14%). PMF solutions assigned primary fine particulate matter to RWC (10%–30%), traffic (25%–40%), and HO (30%–60%), the latter likely reflecting high sulfur emissions from older furnaces and fast secondary chemistry. Despite cold and dark conditions, secondary processes impacted many trace gas and particle species' budget by ±10%–20% and more in some cases. Transport of O_3-rich regional air into Fairbanks contributed to aging, specifically NO_3 radical formation. This work highlights a long-term trend observed in Fairbanks: increasing traffic and decreasing RWC relative contributions as total pollution decreases. Fairbanks exports a relatively fresh pollutant mixture to the regional arctic, the fate of which warrants future study.

Plain Language Summary Fairbanks, Alaska suffers from poor air quality in the wintertime, historically due to a combination of woodstove use for home heating and strong temperature inversions. To better understand this wintertime air pollution, we collected measurements of over 40 gases and particulate matter at a house in Fairbanks. Aromatic gases, a type of volatile organic compounds (VOCs), such as cancer-causing benzene, accounted for about 50% of total measured VOCs. The wintertime burden, or total amount, of VOCs was much higher than other urban areas such as New York City. We found that traffic was the largest source of aromatic VOCs, as well as the regulated air pollutants carbon monoxide and nitrogen oxides. Wood burning was responsible for a large amount of important oxygen-containing gases, while most of the fine particulate matter was from using fuel oil to heat homes. We show that chemistry is responsible for 10%–20% of many pollutants' total. This work highlights a long-term trend observed in Fairbanks: while air pollution steadily declines, due to environmental regulations, traffic is becoming more important and wood heating less so.

Project administration: Robert J. Yokelson, Gianluca Pappaccogli, Stefano Decesari, Becky Alexander, Brent J. Williams, Barbara D'Anna, Jochen Stutz, Kerri A. Pratt, Peter F. DeCarlo, Jingqui Mao, William R. Simpson, Lu Hu
Resources: Robert J. Yokelson, Gianluca Pappaccogli, Stefano Decesari, Becky Alexander, Brent J. Williams, Barbara D'Anna, Jochen Stutz, Kerri A. Pratt, Peter F. DeCarlo, Jingqui Mao, William R. Simpson, Lu Hu
Software: Damien T. Ketcherside
Supervision: Robert J. Yokelson, Gianluca Pappaccogli, Stefano Decesari, Becky Alexander, Brent J. Williams, Barbara D'Anna, Jochen Stutz, Kerri A. Pratt, Peter F. DeCarlo, Jingqui Mao, William R. Simpson, Lu Hu
Validation: Damien T. Ketcherside, Robert J. Yokelson, Philip K. Hopke
Visualization: Damien T. Ketcherside, Lu Hu
Writing – original draft: Damien T. Ketcherside, Robert J. Yokelson, Philip K. Hopke, Lu Hu
Writing – review & editing: Damien T. Ketcherside, Robert J. Yokelson, Vanessa Selimovic, Ellis S. Robinson, Brice Temime-Roussel, Amna Ijaz, Jonas Kuhn, Allison Moon, Gianluca Pappaccogli, Stefano Decesari, Becky Alexander, Brent J. Williams, Barbara D'Anna, Jochen Stutz, Kerri A. Pratt, Peter F. DeCarlo, Jingqui Mao, William R. Simpson, Philip K. Hopke, Lu Hu

1. Introduction

Fairbanks, Alaska (64.8 N, −147.7 W, metropolitan area population ∼95,000 per 2020 Census) has a long history of air quality issues and gradually effective mitigation strategies. In the 1970s, the main concern was frequent wintertime violations of the 9 ppmv CO standard. Violations of the CO standard have not occurred since the early 2000s due to improvements in automotive technology and effective mitigation of the emissions from wood burning for home heating (Simpson et al., 2024 and references therein). Subsequent efforts focused on compliance with the standard for $PM_{2.5}$ (particulate matter with an aerodynamic diameter <2.5 microns) with some success mainly by targeting wood burning (aka residential wood combustion, RWC). Other measures to improve air quality have involved reducing allowed sulfur content in oil for commercial and residential furnaces, power plants, and vehicles. Eighty percent of on-road diesel had to be ultralow S (15 ppm S) as of 1 October 2006 and all by 1 January 2010. Nonroad diesel vehicles had to be ultralow S starting on 1 January 2010 and completed by 31 December 2013. All new heavy duty diesel trucks had to have particle regenerative traps (CRTs) as of 1 July 2007 and selective catalytic reduction systems (SCRs) as of 1 January 2010 (Office of Transportation and Air Quality, 2016).

From early January to 25 February 2022, the Alaskan Layered Pollution and Chemical Analysis (ALPACA) campaign took place in Fairbanks with an unprecedented level of instrumentation and chemical/physical/meteorological detail (Simpson et al., 2024). Placed on the timeline of the evolving Fairbanks airshed, the intensive observation period of the ALPACA campaign took place during the COVID-19 pandemic, which may have increased home heating needs and reduced traffic to some extent. In addition, 6 months after the campaign, the sulfur standard for heating oil was lowered (https://dec.alaska.gov/air/anpms/communities/fbks-pm2-5-fuel-switch-requirement/), which has apparently already significantly reduced ambient SO_2 (http://alpaca.alaska.edu).

Previous Fairbanks air quality studies have mostly focused on $PM_{2.5}$ to inform mitigation strategies. One of the larger, previous Fairbanks air quality studies sampled $PM_{2.5}$ for 8 winters (2005/6–2012/13) at 7 sites (Ward, 2013). A chemical mass balance (CMB) source apportionment using profiles measured for local fuels found that either woodsmoke or heating oil was the main source of $PM_{2.5}$ at each site. Sulfate and nitrate were important sources while traffic was not detected or insignificant. However, a follow-up study using additional analyses of the same filter samples suggested that CMB significantly overestimated woodsmoke (Busby et al., 2016). Receptor modeling of a large data set from 2005 to 2012 found that woodsmoke accounted for 39.6% of $PM_{2.5}$ in winter, while the sum of sulfate, diesel, and nitrate accounted for 48% (Wang & Hopke, 2014). Later, using 2013–2019 data, Ye and Wang (2020) found that the relative importance of woodsmoke and diesel had decreased compared to earlier work, while secondary aerosol had increased in importance. Their three largest wintertime $PM_{2.5}$ sources were sulfate (44%), combined gasoline and diesel (21%), and woodsmoke (17%). During winter 2020, particulate sampling in the Fairbanks area again identified sites dominated by either woodsmoke or distillate oil combustion emissions (Simpson et al., 2020). In the previous 10 years leading up to the ALPACA study, the estimated vehicle miles traveled in the Fairbanks/North Star borough (FNSB) increased by ∼36% (private communication, Scott Vockeroth, Alaska DOT), and in the 20 previous years, the borough population increased by ∼14%, while the number of registered vehicles decreased by under 2% (https://dmv.alaska.gov/research-statistics/research-statistics/). The borough's current, ongoing woodstove conversion program had removed or converted 3,576 woodstove or other solid fuel-fired heating devices in the FNSB nonattainment area as of 22 November 2023 (https://www.epa.gov/newsreleases/epa-finalizes-action-fairbanks-air-plan-partners-state-new-one-provides-10-million, https://www.fnsb.gov/386/Change-Out-Programs) and a public utility has worked to replace distillate oil with natural gas for home heating (https://www.interiorgas.com/our-mission/). In this study, we employ the ALPACA data to provide a detailed description of the air quality in a Fairbanks residential neighborhood in January–February 2022. Then, we compare to other sites in Fairbanks and investigate the sources of 45 trace gas and particulate species using diel cycles and positive matrix factorization (PMF).

2. Materials and Methods

2.1. Site Descriptions and Data Collected

Four heavily instrumented sites provided the bulk of the ALPACA data as described in full detail in an overview paper by Simpson et al. (2024). A National Core monitoring site (NCore) has been operated continuously since 2009 by the Alaska Department of Environmental Conservation (ADEC) for the USEPA. Another monitoring site

was established, 580 m south of NCore, for the duration of the ALPACA campaign at the Community Technical College (CTC). The State Building located about 50 m from CTC is where much of the literature data on Fairbanks was collected and all three of these sites are considered representative of downtown. Some trace gas data and the bulk of the meteorological profiles were collected at the University of Alaska Fairbanks (UAF) farm 6 km west of downtown. This study focuses mainly on the outdoor data collected at a house in a residential area (Hamilton Acres subdivision) ∼1.75 km northeast of CTC where both indoor and outdoor air was studied via switching inlets. The A-street regulatory site collected outdoor $PM_{2.5}$ and some meteorological data ∼0.6 km southwest of the house. During the ALPACA campaign, a mobile lab with $PM_{2.5}$ measurements sampled much of the Fairbanks urban area and Birch Hill, which was ∼3 km northeast of the house (Fig. 2 in Simpson et al., 2024) with the goal of characterizing spatial variability (Robinson et al., 2023). We will make brief comparisons between sites and the mobile lab to explore how representative each site may be of the overall Fairbanks urban area.

2.2. Instrument Descriptions

All the sites, mobile lab results, instrumentation, sampling strategies, and most of the calculations pertinent to this study have been described in full previously (see the site map in Brett et al., 2025; Edwards et al., 2024; Robinson et al., 2023, 2024; Simpson et al., 2024; Yang et al., 2024). Here, we first briefly summarize instruments that collected data at one-minute time resolution outdoors at the house site. A proton transfer reaction time of flight mass spectrometer (PTR-TOF-MS 4000, Ionicon Analytik) provided calibrated (with a few exceptions noted below) measurements of (in ascending mass order) methanol, propyne, acetonitrile, acetaldehyde, formic acid, ethanol, butene, methanethiol, acetone, acetic acid, furan, isoprene (this mass impacted by fragments, vide infra), methyl vinyl ketone plus methacrolein, methyl ethyl ketone, hydroxyacetone, benzene, methyl furan, pentanone, toluene, furfural, maleic anhydride, hexanone, C8 aromatics, methyl furfural, C9 aromatics, naphthalene, C10 aromatics, monoterpenes, and D5-siloxane. Numerous other masses were monitored, but not calibrated, so mixing ratios were estimated as described elsewhere (Permar et al., 2021; Sekimoto et al., 2017). Ozone was measured by NO titration in a scrubberless ozone monitor (2B Tech Model 211), and NO, NO_2, and NO_x were measured by UV absorption (2B Tech Model 405), which are further described in Selimovic et al. (2020). Formaldehyde (HCHO), CO, CO_2, and CH_4 were measured by cavity ring down spectroscopy (CRDS, Picarro models G2307 and G2401).

Additionally, a high-resolution time-of-flight aerosol mass spectrometer (HR-TOF-AMS, hereinafter AMS, Aerodyne Inc.) was used to monitor submicron organic aerosol (OA), sulfate (SO_4), particle nitrate (pNO_3), ammonium (NH_4), and chloride (Chl) and these species were summed to obtain total nonrefractory submicron mass (TNRM). The AMS SO_4 measurements are potentially impacted by positive interference described next. $SO_{2\ (aq)}$ generates sulfite (SO_3^{2-}) and bisulfite (HSO_3^-) in aerosol liquid water, both of which can form an adduct with HCHO (hydroxymethanesulfonate, HMS) and potentially other aldehydes (Dingilian et al., 2024). These adducts are S(IV) compounds and they and other organosulfur compounds can be significant particulate species. The extent to which these non-SO_4 compounds are detected as SO_4 by the AMS is the subject of on-going work. Ion chromatography (IC) of filter samples can separate SO_4 and some S(IV) species (Dingilian et al., 2024). The ALPACA campaign average ratio of S(IV) to SO_4 in the $PM_{0.7}$ at CTC on a per sample (12hr or 24hr) basis was measured by IC as 0.16 ± 0.13 (range 0.02–0.58) and the campaign total ratio was 0.21 (Moon et al., 2024). Black carbon (BC) was measured with an aethalometer (Model AE33, Aerosol Magee Scientific) and $PM_{1.0}$ was estimated as the sum of BC + TNRM.

At the house site, the PTR-TOF-MS VOCs, NO_x, and O_3 measurements shared an inlet system. An inlet switch was used to transition between two heated inlets, one for indoor air and the other for outdoor air every 10 min. This switch consisted of two electronic 1/4″ PTFE three-way valves. Additionally, a continuous-flow bypass was included in the design to facilitate a quick instrument response during switching. One minute of data on either side of an inlet transition was removed to limit the measurement of mixed indoor and outdoor samples and an extra minute was removed for the "sticky" species such as formic and acetic acid (Müller et al., 2016; Permar et al., 2023; Yokelson et al., 2003). Data points that deviated from consecutive measurements for a short period of time (1 min) were also removed. All other measurements listed above (notably AMS, CRDS HCHO, and CO) were taken via a separate, nonheated switching inlet system. While we attempted to synchronize indoor/outdoor switching of the two inlet systems, this was not always possible. Therefore, there were moments when PTR-TOF-MS VOCs, NO_x, and O_3 were being sampled indoors while the CRDS HCHO, CO, CO_2, CH_4, and particles were being sampled outdoors.

With six exceptions, the PTR-TOF-MS VOC species listed above were calibrated in the field using four certified gas standards that were also shared for cross-calibration with the PTR-TOF-MS (PTR-TOF 6000 X2, Ionicon Analytik) deployed at the CTC (Fairbanks downtown) site (Ijaz et al., 2024; Simpson et al., 2024). At the house site, formic and acetic acid were quantified using a humidity-dependent sensitivity function derived from liquid calibrations performed prior to deployment. D5-siloxane mixing ratios were quantified using a sensitivity derived from a gas standard calibration postdeployment. Sensitivities for maleic anhydride, methanethiol, and naphthalene were assumed to be the same as our previous theoretical calculations (Permar et al., 2021). A condensation particle counter (CPC) was installed at the house site on 11 February 2022 that used butanol and diethylene glycol as solvents with a liquid exhaust line routed to the outside. Due to the fragmentation of butanol and diethylene glycol, there was substantial interference with two VOC species, propyne and butene, in the outdoor data and they were not included in the analyses described below.

2.3. EPA PMF5.0 Model Setup, Sensitivity, and Performance

To run EPA PMF5.0, the user provides the observations as a matrix of i samples (in time order in the rows) by j species (the time series of each species is a column). The user also provides the best estimate of the uncertainties for each species and a provisionally selected number (n) of factors. PMF5.0 solves for the n fixed factor concentration profiles (dimensions $j \times 1$) and the matrix (dimensions $i \times n$) of the factor contributions to the fit for each sample that best fit the observations as determined by minimizing an objective function Q. PMF5.0 also calculates the factor contributions to the total fit signal for each of the j species and a great deal of diagnostic and other useful information. The user assigns factors to real-world sources based mostly on similarity of the factor profile to the concentration profile of known sources (ideally locally measured), but the time series or diel cycle of the factor contributions to each sample and other characteristics can support assignments. A major goal is to determine the number of factors n such that the data are optimally fit by factors with well-supported assignments. This process commonly involves test runs to determine the impact of selecting different model options or reasonable potential adjustments to the model input. We summarize our test run results in this section and our best solutions in Section 3.3. Complete documentation for EPA PMF5.0 is available online (Norris et al., 2014). It should be noted that this PMF analysis was conducted using the bulk chemical properties observed by AMS rather than individual ions.

We expect that emissions from the same source will often vary together and PMF solves for factor profiles based largely on the covariance of species in the mixture. Thus, we examined the possible impact of the house sampling system on the PMF results. Because the indoor/outdoor switchings on the two inlet systems at the house were sometimes out of phase, there were some 1-min samples when the VOC-NO_x-O_3 inlet system (hereinafter "inlet A") could potentially respond to a brief outdoor signal from a source without concurrent monitoring on the PM-CO-HCHO inlet system (hereinafter "inlet B") and vice versa. In addition, we found that gases measured on inlet A helped assign factors to RWC, traffic, and other sources, while the particulate profile (especially sulfate) measured on inlet B helped assign factors to heating oil and other sources. The nature of the sampling setup is, in part, why we ultimately filtered the available concentration/time series data four different ways as described next. This allowed us to determine if the selection of input data strongly affected the PMF results and overall uncertainty by, for example, impacting sampling coverage or covariance. It should be noted that any time-based averaging was done using the 1-min resolution data. For example, the average of hour 0000 LT includes all relevant and available data collected between 00:00 LT and 00:59 LT.

- Input data set #1 included all the inlet A outdoor data (e.g., VOCs, O_3, NO_x), but only the inlet B outdoor data (e.g., AMS species, CO, HCHO) when inlet A was also sampling outside. This filtering was selected arbitrarily and analyzed with PMF first, mostly at 1-hr averaging with four to seven factors selected. A strong 6-factor solution is described in Section 3.2.
- Input data set #2 was created next and included all the outdoor data from both inlet systems resulting in about 20% more data from inlet B including some high signal levels. BC and $PM_{1.0}$ from inlet B and methanethiol and naphthalene from inlet A were only verified and included when forming input data sets #2 and #3. Input data set #2 was built at numerous different time resolutions ranging from 1 minute to 6 hours and also analyzed by the PMF model with the selected number of factors ranging from 6 to 15.
- We also did model runs with input data set #2 at 1 hr time resolution after truncating the warm event at the end of the campaign since the warm event may introduce new sources via enhanced vertical mixing or be less

Table 1
Summary of Species Used for Factor Assignments and Selected Model Performance Data

# Factors	4	5	6	7
Q(robust)	96,819.0	76,996.9	62,270.3	50,030.1
Pred *v* Obs Σslopes, Σr^2	26.2, 26.2	28.1, 27.6	29.0, 28.5	29.8, 29.3
BS-DISP phase swaps	–	0	0	3
O_3	O_3	O_3	O_3	O_3
NO_2, secondary PM	Aged	Aged	Aged	Aged
BB long-lived VOCs	BB-LL	BB-LL	BB-LL	BB-LL
Aromatics, NO, CO	Mostly FF	Traffic	Traffic	Traffic 1
Sulfate		Space heating	Heating oil (HO)	Heating oil
BB short-lived VOCs (Furans)			BB-SL	BB-SL
Aromatics				Traffic 2

Note. When decreasing the number of factors from six to five, the heating oil and short-lived BB VOCs factors merge into a single indoor heating factor. Decreasing to four factors merges the indoor heating and traffic factors to a single mostly "fossil fuel" factor that includes a BB contribution. Increasing the number of factors from six to seven splits the traffic factor into two factors that sum to the single 6-factor solution traffic factor profile.

representative of winter due to warmer temperatures and longer days. A 9-factor PMF solution for the truncated input data set #2 time series is also described in Section 3.2.

- Input data set #3 included only data measured when both inlets A and B were simultaneously sampling outdoors but consistently led to PMF results at various averaging times within the range obtained with the other input data sets.

We summarize potential impacts of the different input data sets on the PMF results from the standpoint of covariance and sampling coverage. Input data set #3 eliminated the possibility of the PMF model considering data measured when only one of the two inlet systems sampled a brief event, but this input data set also used the least data per hour when computing, for example, hourly averages, which could negatively impact the characterization of longer-lasting events. Conversely, input data set #2 used the most data to characterize any averaged time period, but it also maximized the potential for measuring a brief event on only one of the inlet systems. Indeed, for many species, the time series contained some brief spikes. Finally, input data set #1 was intermediate for both sampling coverage and quantifying covariance between species measured on different inlet systems.

An additional goal was to include as many species as possible in the PMF analyses, but we eliminated propyne and butene (CPC outlet interference) and NH_3, which was measured on a third inlet and had low correlation with all other species (Table S1 in Supporting Information S2). Eliminating NH_3 was disappointing because the EPA 2017 National Emissions Inventory (NEI) reports that the US national average NH_3/SO_2 molar ratio for heating oil combustion emissions is ~0.5 (Belova et al., 2022). Thus, in addition to its general atmospheric significance, it could have been useful for factor assignment.

We first focused on determining the optimum number of factors by running EPA PMF5.0 using the 41 or 45 remaining gas phase and particulate species for 865 samples in the case of hourly averages. The uncertainty matrix is calculated in the program and is a function of the error fraction (measurement uncertainty) and the method detection limits. Error fractions for calibrated VOCs ($n = 26$) were set to 10%, and noncalibrated species' ($n = 2$) error set to 50%. Solutions were obtained for 4–15 factors and compared based on how confidently the factor profiles could be assigned to real-world sources, fit quality, and the error analysis provided by bootstrapping (BS), displacement (DISP), and BS-DISP (Paatero et al., 2014) following the software manual (Norris et al., 2014). We selected six factors as optimum for input data set #1. As shown in more detail in Sect. 3 and Table 1 after we have introduced the factor assignments, for data set #1, moving to the 7-factor solution (from the 6-factor solution) sharply increased the number of factor swaps and sources appeared to be unnecessarily split. The 5-factor solution (compared to the 6-factor solution) forced unrealistic consolidation of emissions very likely from different sources (Table 1).

Once the 6-factor solution was chosen as optimum for input data set #1, numerous exploratory runs with six factors tested the effect of various PMF model run options as an ad hoc sensitivity analysis. For instance, methanol and ethanol had numerous sharp peaks in their mixing ratio time series that were not fit well and they were the least well-fit major gases overall. Previous work has shown that these species are difficult to incorporate in PMF due to the large number of emissions sources (Gkatzelis et al., 2021). Deleting these two species from the input file as a test eliminated them from the factor profiles, but otherwise had little effect on factor profiles and assignments or factor contributions to the other fit species. CO_2 and CH_4, were well fit, but abundant in background air and removing these two gases from the input data as a one-off test also had little effect on the results. After establishing low model sensitivity to the presence or absence of these four species, we retained them in subsequent runs. EPA PMF5.0 displays the signal to noise for each species and gives the user an opportunity to adjust the uncertainties before seeking a solution by running the model. Our PMF results were not very sensitive to these adjustments. Even designating methanol and ethanol as "weak" species and thus increasing their uncertainty by a factor of 3 had little effect on the results. We mostly adopted the model recommendations for uncertainty changes. Model options for handling missing data points include eliminating entire samples when any species was missing or replacing missing data points for individual species with the species-specific campaign median and also assigning the point an uncertainty equal to four times the median value to down-weight its impact on the overall results (Polissar et al., 1998). The first option removed more than 50% of the input data but resulted in factor assignments and factor contributions that were very similar to the second option, which was our default. In addition, PMF runs with 100 iterations of the model (to ensure avoiding a local minimum in Q, the goodness of fit parameter) gave results essentially identical to PMF runs with 20 iterations. We verified that none of the outdoor methanol and ethanol peaks coincided with indoor experiments at the house. We did not note any evidence of any VOC concentration events/trends inside the house impacting the outdoor data.

We provide a general assessment of model performance next and discuss some aspects in more detail in Section 3. The slopes and r^2 in predicted versus observed scatter plots, the ratio of total fit signal to total measured signal, and scaled residuals were generally good (slopes and ratios 0.7–1.0, average $r^2 \sim 0.75$, scaled residuals mostly normally distributed and within ±3). The lowest performance and the largest scaled residuals were for methanol and ethanol, which was readily traced to the fact that, as noted above, these two VOCs presented numerous sharp peaks and the predicted versus observed time series showed significant underpredictions at the tip of each of these peaks. These underpredicted points shifted the slopes in the predicted versus observed scatter plots (unforced intercepts) to around 0.7, but the large majority of points did lie along the 1:1 line and 82%–92% of the total measured amount of these alcohols was fit.

2.4. Furnace Exhaust Measurements

To aid in factor identification of HO sources, we collected a single sample of the house's heating oil furnace exhaust. The inlets were lofted just above the exhaust pipe on the roof for ∼30 min at the end of the field campaign. The cyclical nature of the furnace ignition resulted in a low frequency of emissions over that course of time. Therefore, a subset of data with clear signals from the furnace exhaust was averaged and used for the ADEC source profile comparison in Section 3.3. Unfortunately, the AMS had difficulty with data collection at the time resulting in a lack of speciated particle data to compare to existing profiles.

3. Results and Discussion

3.1. Overview of Trace Gas Observations

Figure 1 shows the time series of a few key measurements for the duration of the ALPACA intensive. Important periods include a prolonged cold spell with a strong surface-based inversion and enhanced pollution centered around 1 February termed the "cold event" by the ALPACA science team (Edwards et al., 2024; Mao et al., 2024; Simpson et al., 2024; Yang et al., 2024). In contrast, enhanced pollution also occurred at the end of the campaign during higher temperatures (the "warm event"). By the end of the campaign, the day length had almost doubled compared to the beginning, from 5.3 to 9.7 hr (Simpson et al., 2024).

In most studied urban pollution scenarios, NO_x, VOCs, and UV light are present in relative proportions that spur aggressive daytime O_3 formation (Finlayson-Pitts & Pitts Jr, 2000; Wu et al., 2024). Additionally, background and secondary O_3 along with OH from the photolysis of O_3, HONO, HCHO, and other carbonyls are the main daytime oxidants driving aggressive secondary chemistry, while O_3 and the NO_3 radical are important nighttime

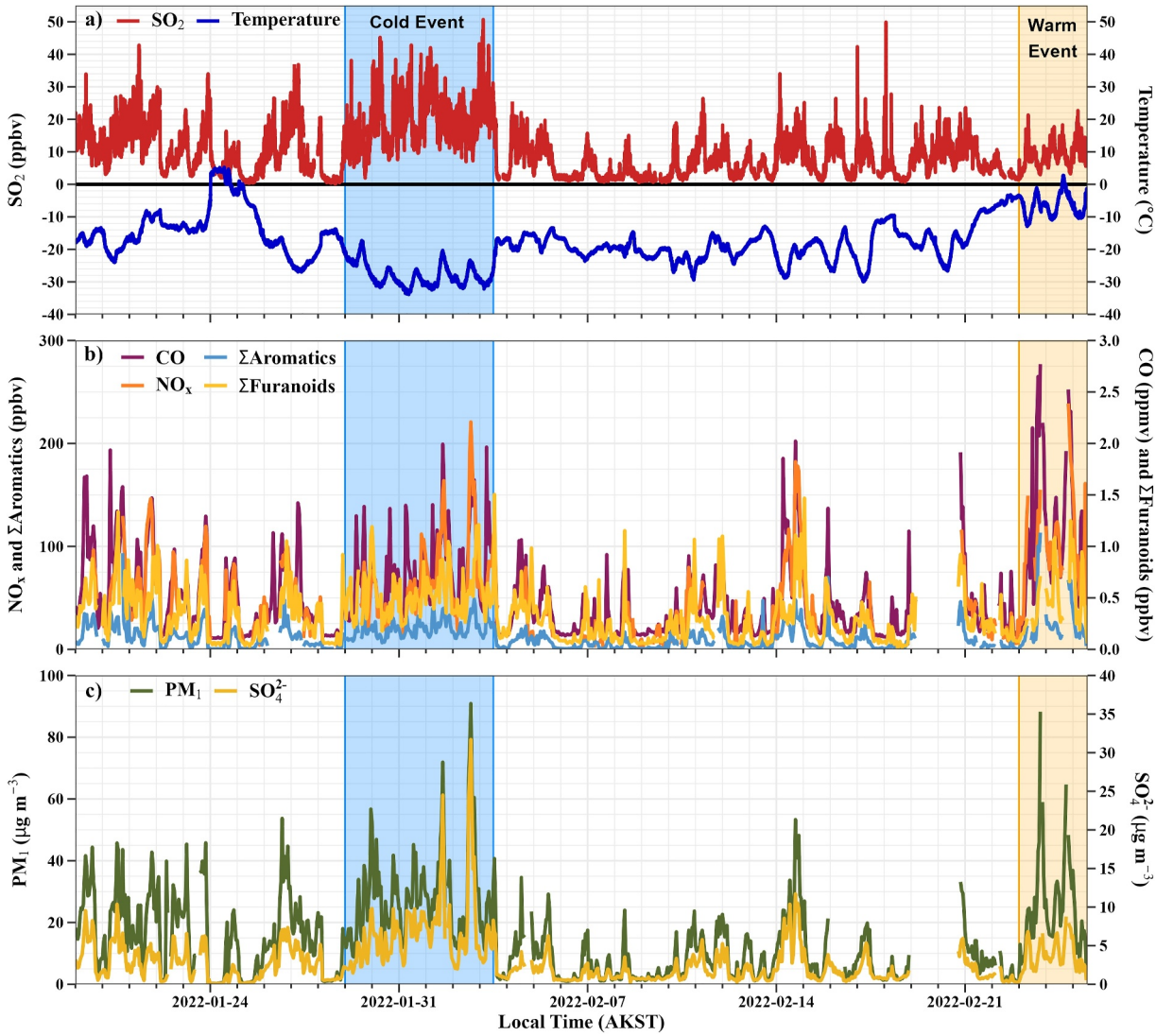

Figure 1. Time series (hourly) of selected key species across the ALPACA campaign. SO_2 and temperature were measured at CTC and the other measurements are outdoors at the house site. Note the increased SO_4 and PM during the cold event and the increase in PM along with NO_x, CO, and aromatics during the warm event.

oxidants. In contrast, during winter in Fairbanks, strong inversions trap very high concentrations of primary pollutants (e.g., $PM_{2.5}$, NO_x, CO, SO_2, and aromatic VOCs) near the surface. In particular, the NO_x concentrations are high enough to quickly titrate surface O_3 concentrations to near-zero (Figure 2a). Surface O_3 can be briefly present at modest mixing ratios (20–40 ppbv) when the inversions break up and relatively cleaner regional background air with some O_3 impacts the surface. The anticorrelation of O_3 with NO_x shown in Figure 2a also occurs between O_3 and other primary pollutants including PM and CO (Figure S1 in Supporting Information S1). Figure 2b shows the coincidence of higher O_3 (up to 50 ppbv) with higher wind speeds from the east or west.

In wintertime Fairbanks, NO_x titration of O_3 leads to NO_3 production, which along with decreased light levels increases the importance of NO_3 as an oxidant relative to O_3 and OH compared to the more commonly studied urban and summertime scenarios. NO_3 production rates ($P(NO_3)$), calculated using the NO_2 and O_3 concentrations and the temperature-dependent rate constant (Burkholder et al., 2020), were sustained in both daytime (average 0.15 ppbv/hr) and at night (average 0.1 ppbv/hr) when NO_3 photolysis is not a factor (Figure 2c). However, NO reacts rapidly with NO_3 to reform NO_2 ($k = 2.6 \times 10^{-11}$ cm^3 $molecules^{-1}$ s^{-1} at 1 atm and 273K) reducing the available NO_3 for reaction with VOCs. Detailed photochemical modeling in a separate paper (Kuhn et al., in preparation) estimates campaign average OH and NO_3 in the surface layer at 3 m above the ground level

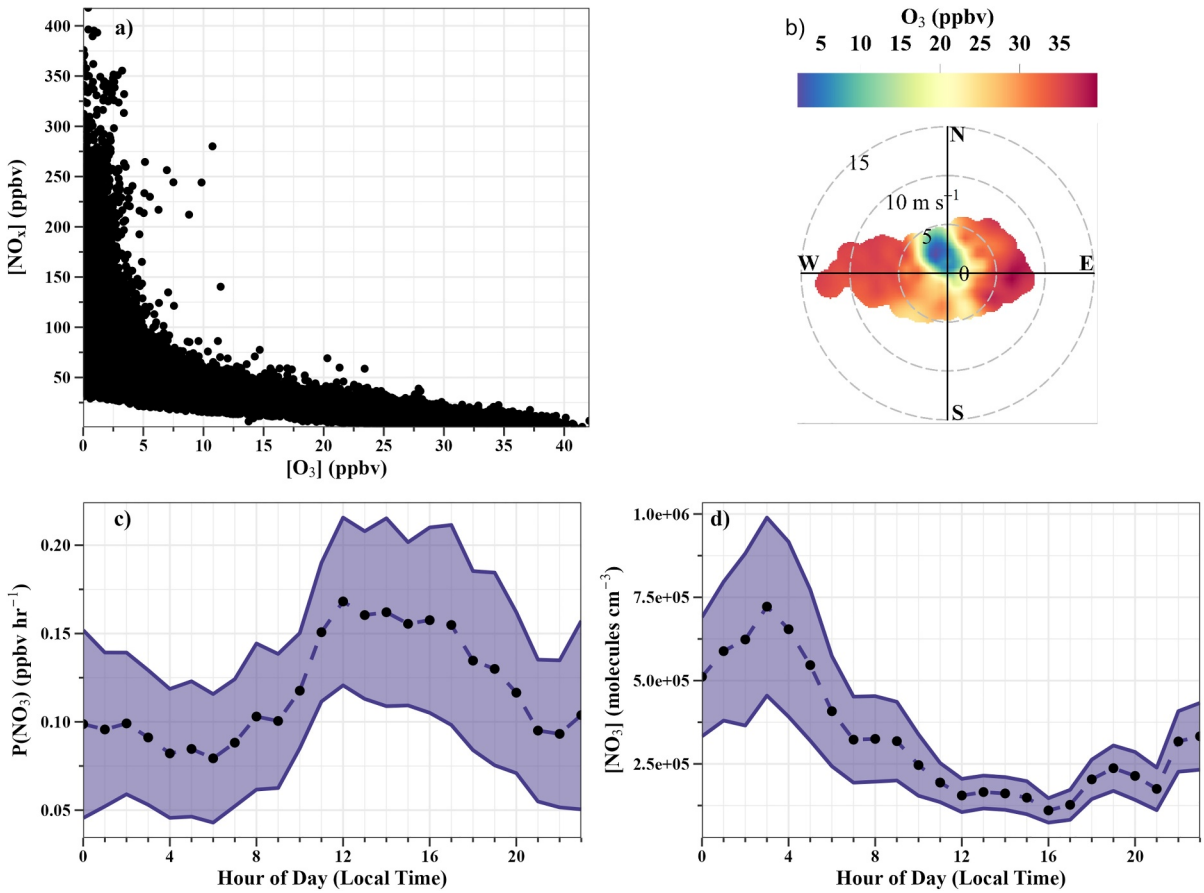

Figure 2. (a) Large concentrations of primary pollutants accumulate near the surface during inversions (e.g., Figure 1; Table S2 in Supporting Information S2). When inversions weaken, mixing with clean regional background air containing some O_3 rapidly reduces the primary pollutant concentrations at the surface and the O_3 is also quickly removed via reaction with NO_x. Thus, surface O_3 is anticorrelated with the primary pollutants. (b) High surface O_3 mainly occurs at higher wind speeds, bringing in regional air from the east or west. (c) Mean (shown as points) ± 95% CI (confidence intervals represented by the ribbon) NO_3 radical production rates. Mixing and the accompanying reaction of O_3 and NO_2 to produce NO_3 can occur throughout the day and night. (d) Mean (shown as points) ± 95% CI (represented by the ribbon) modeled NO_3 concentrations are higher at night when the emission of reactive VOCs by local RWC peaks (vide infra).

as 7.5×10^4 and 7.1×10^5 molecules cm^{-3}, respectively (Figure 2d). For VOCs that react quickly with NO_3 (e.g., 2,5-dimethyl furan, $k = 5.8 \times 10^{-11}$ cm^3 $molecules^{-1}$ s^{-1} at 1 atm and 273K), this corresponds to lifetimes of ~7 and 29 hr with respect to NO_3 and OH although the NO_3/OH ratio is likely higher than average at night when some of these VOCs are mainly emitted (Figure 2d). NO_3 is more abundant above the surface where NO concentrations are lower. Model estimated campaign averages from 0 to 200 m for NO_3 and OH are 4.74×10^6 and 4.24×10^4 molecules cm^{-3}, respectively, corresponding to dimethylfuran lifetimes of one and 50 hr for NO_3 and OH. Note that the different and varying vertical distributions of NO_3, OH, and dimethylfuran within the lower 200 m (due to surface layer changes) introduce some uncertainty to this estimate. However, it implies that any vertical mixing will tend to increase the importance of NO_3 as an oxidant.

The decreased importance of OH and O_3 oxidation in Fairbanks in winter is also manifested in the average historically measured wintertime "sulfur oxidation ratio" (SOR, the percentage of fuel S converted to sulfate) of 6% (Simpson et al., 2020). During ALPACA, the isotopic composition-based SOR at CTC was 8 ± 4% (Moon et al., 2024). While not an equivalent calculation, the mass ratio of N in pNO_3 to N in NO_x at the house site was even smaller at 1.7%, consistent with a small degree of oxidation of these primary pollutants. Note, however, that processing a small fraction of these combustion-generated precursors to PM can have significant local impacts given the large amount of emissions and persistent inversions.

Figure 3 shows the diel cycles of NO_x, CO, and selected aromatic VOC and furanoid mixing ratios at the house. The time series, events, and diel profiles help identify the factors influencing surface air quality during the

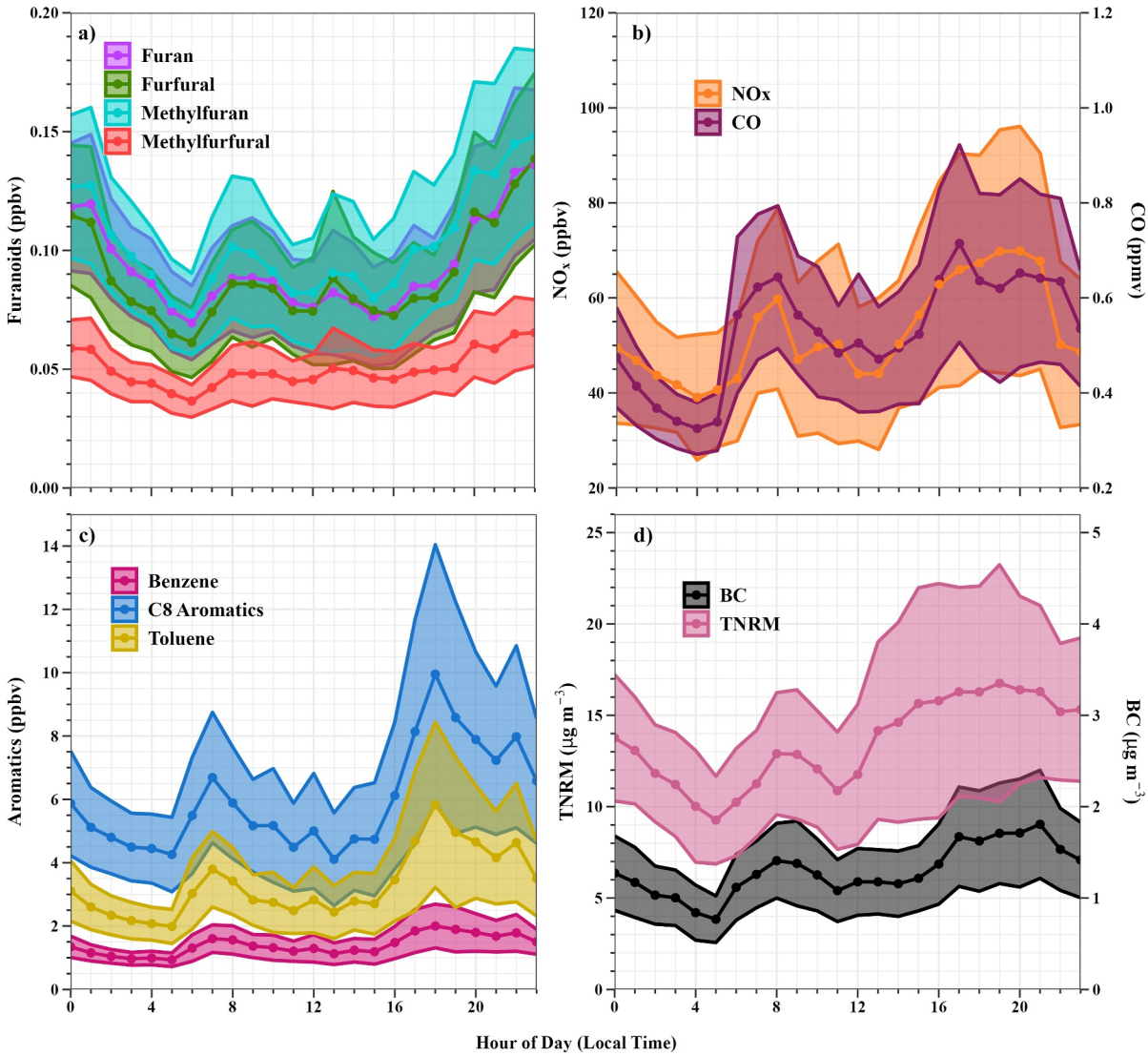

Figure 3. (a) The diel cycles (mean ± 95% CI) for the reactive, short-lived furanoids peak in the middle of the night, consistent with a nearby RWC source. (b–c) The diel cycles for NO_x, CO, and aromatics have peaks consistent with a rush-hour traffic contribution. (d) BC and TNRM also have rush hour peaks, but they are smaller relative to an elevated baseline, consistent with traffic being one of several sources of these species. Note that TNRM rises quicker than BC after 11 AM, consistent with secondary aerosol formation.

campaign as noted throughout the discussion. The rush hour peaks for NO_x, CO, and aromatic VOC mixing ratios suggest a traffic source as is revisited below. The furanoids peak in the middle of the night, reflecting the impact from local wood-burning sources (Gilman et al., 2015).

To explore variability across the fixed sites and help assess the representativeness of each fixed site, we present the campaign average mixing ratios or mass concentrations for many trace gas and particulate species at the various Fairbanks sites during ALPACA in Table S2 in Supporting Information S2. The campaign average mixing ratios for O_3, CO_2, and CO at CTC were within +4%, −2%, and −10%, respectively, of the average mixing ratios at the house site and NO_x was about 25% higher at CTC. The average VOC mixing ratios were similar at the house site and CTC with just C8 and C10 aromatics, ethanol, hydroxyacetone, and pentanone being more than 50% lower at CTC and just acetonitrile and maleic anhydride (both associated with biomass burning (BB)) being more than 50% higher at CTC when considering 26 comeasured VOCs (Table S2 in Supporting Information S2). The slope and coefficient of correlation for numerous species pairs, both at individual sites and for the same species measured at different sites, are shown in Table S1 in Supporting Information S2 and can be used for more comparisons and to help assess the degree of mixing (Brett et al., 2025). The lowest path of the UCLA DOAS

system passed above the house and measured a campaign average 28.45 ± 16.45 ppb of NO_2, about 1.4 times higher than the house site average, but almost identical to the CTC site average. Part of any discrepancy can be due to data gaps and the partitioning between NO and NO_2. The lowest DOAS path reported an average (± standard deviation) HCHO of 1.89 ± 1.63 ppb, about 36% higher than the house site and just 5% lower than CTC. The average $PM_{2.5}$ and BC mass concentrations measured near the house by the mobile lab were about 11% and 7% higher, respectively, than the average values measured by the fixed instruments at the house (Robinson et al., 2023; Table S2 in Supporting Information S2). A more detailed analysis of spatial variation can be found in Robinson et al. (2023).

At the house, the sum of the 28 mostly calibrated PTR-TOF-MS VOCs listed above (Section 2.2) plus the CRDS HCHO accounted for 94 ± 6% of the total raw VOC signal (normalized counts per second) generated by the 313 peaks in the full PTR-TOF-MS mass spectrum. The campaign average mixing ratio for the sum of these 29 VOCs was 32.7 ± 25.0 ppb (range of 1h averages, 4.3–177 ppb). We refer to the sum of these 29 VOCs as "total VOCs" (TVOC) but is considered a lower limit due to the unreported VOCs from the PTR-TOF-MS and alkanes, which were not measured in ALPACA, but likely account for 5%–25% of the true total VOC budget (Heald et al., 2008, 2020). C8 aromatics were the most abundant VOCs measured at the house site during ALPACA, followed by methanol and ethanol (Table S2 in Supporting Information S2). The sum of the 5 measured aromatics plotted versus TVOC had a slope of 0.50 and high r^2 (0.88), showing the aromatics accounted for about one-half of measured TVOC at the house (Figure 4a, Table S1 in Supporting Information S2). The mean mixing ratios of the aromatics at the house in the decreasing order of abundance were C8 aromatics (5.98 ± 6.39 ppb), toluene (3.32 ± 3.92 ppb), benzene (1.41 ± 1.31 ppb), C9-aromatics (1.00 ± 1.11 ppb), and C10-aromatics (0.21 ± 0.23 ppb; Table S2 in Supporting Information S2). The order of abundance for aromatics at CTC differed in that toluene was the most abundant (2.30 ± 3.50 ppb), followed by C8 aromatics (1.90 ± 2.01 ppb). Four aromatic trace gases were measured at the UAF farm (Table S2 in Supporting Information S2), which was impacted by a downslope flow of cleaner air from the north. At the UAF farm, the sum of ethylbenzene (0.17 ± 0.17 ppb) and xylenes (0.51 ± 0.41 ppb) represents the C8 aromatics (0.68 ± 0.44 ppb), followed by toluene (0.41 ± 1.10 ppb) and benzene (0.22 ± 0.24 ppb), similar to the order at the house (Table S2 in Supporting Information S2). The mean mixing ratios for aromatics at the farm were about six to eight times lower than at the house and about three to six times lower than at CTC. The average toluene/benzene ratio (1.86) was the lowest at the farm. Thus, the aromatic profile is not uniform across Fairbanks and the variability between the three sites likely reflects differences in the local traffic and heating mix as well as more aging and dilution at the farm.

At the house, all the aromatics were highly correlated with each other (Table S1 in Supporting Information S2) and all the aromatics were also highly correlated with CO (r^2 range 0.86–0.92, Table S1 in Supporting Information S2). In turn, TVOC (ppb) plotted versus CO (ppm) had a slope of 50.3 ($r^2 = 0.79$, Figure 4b, Table S2 in Supporting Information S2), much lower than usually observed for biomass burning (e.g., 127–150 ppb ppm^{-1}, Gkatzelis et al., 2024; Permar et al., 2021). CO plotted versus CO_2 had a slope of 0.0095 and r^2 of 0.76, indicating that these two gases are primarily produced by fossil fuel combustion that is more efficient than RWC, which produces CO/CO_2 molar ratios in the range of 5%–10% (Fachinger et al., 2017; Traviss et al., 2024; Ward, 2013). The summed aromatics versus NO had a slope of 0.297 ($r^2 = 0.61$). These slopes and correlations, along with the diel cycles (Figures 3b and 3c), are consistent with traffic as a major source of TVOCs, aromatic VOCs, CO, and NO_x. Aromatic VOCs are also produced by wood burning. The toluene/benzene ratio is typically <1 for wood burning (Traviss et al., 2024; Fig. 5a in Zhang et al., 2016) and in the range of 1–10 for vehicles (Marques et al., 2022; Fig 5a. in Zhang et al., 2016 and references therein). One sample of the house oil furnace exhaust had a toluene/benzene ratio of 1.75 (Table S3 in Supporting Information S2). The overall average toluene/benzene ratio outdoor at the house site was 2.89 ($r^2 = 0.93$), consistent with a dominant traffic source (Figure 4c) and thus smaller contributions from other sources. The nighttime peak in aromatics about 0.25–0.5 the size of the rush hour peaks (Figure 3c) was likely from heating oil combustion and RWC. Furthermore, the toluene/benzene ratio decreases overnight (Figure S2 in Supporting Information S1), reflecting a shift in sources.

Two alcohols, methanol and ethanol, were the second and third most abundant VOCs at the house with mean mixing ratios of 5.57 ± 5.66 and 5.31 ± 4.28 ppb, respectively. The sum of the two alcohols plotted versus TVOC had a slope of 0.344 ($r^2 = 0.826$). The source of these two species warrants more investigation. They correlate well with gases identified with traffic and may reflect the use of windshield and gas-line antifreeze for vehicles. Note that Alaskan gasoline products do not feature added ethanol; thus, the data presented here provide a unique constraint on nontraffic ethanol emissions (e.g., VCPs) that is difficult to ascertain in other, more densely

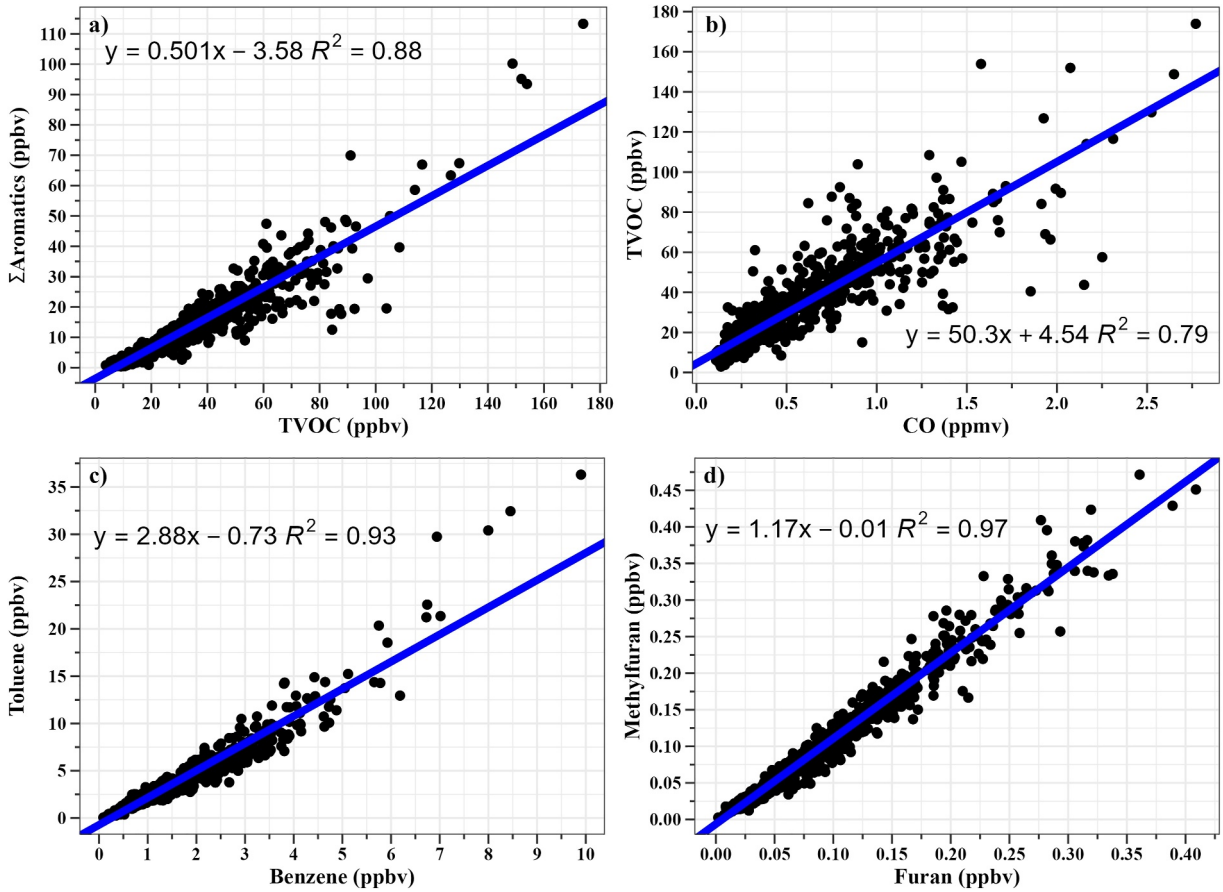

Figure 4. Scatter plots using 1-hr time resolution data and linear regression. (a) Aromatic VOCs account for about 50% of total measured VOCs in Fairbanks during ALPACA. (b) The ratio of total VOCs to CO is consistent with a large contribution from fossil fuel combustion as opposed to biomass burning. (c) The toluene to benzene ratio is most similar to the toluene to benzene ratio of traffic sources. (d) Typical high correlation between furanoid species (See also Table S1 in Supporting Information S2).

populated urban areas. Ethanol could have a contribution from personal care products (Gkatzelis et al., 2021) and it correlated slightly better on average with aromatics (r^2 range 0.77–0.85) than it did with methanol (r^2 = 0.77). Methanol correlated better with aromatics than OVOCs typically from RWC as listed earlier in this section (Table S1 in Supporting Information S2).

The above results for TVOCs, aromatics, and alcohols can be compared roughly to wintertime VOC measurements made in Boulder, CO 1–18 February 2018 and New York City (NYC) 5–28 March 2018 by Gkatzelis et al. (2021). They report their campaign median mixing ratio *fit* by PMF for the sum of 165 VOCs that does not include methanol, HCHO, or alkanes as 13.11 ppb for NYC and 4.49 ppb for Boulder. Our ALPACA TVOC median *observed* mixing ratio after subtracting methanol and HCHO is 20.21 ppb, which is 54% higher than NYC and 4.5 times greater than Boulder. The high TVOC mixing ratios in Fairbanks are likely due, in large part, to the strong, shallow inversions. The median fit mixing ratio for the sum of benzene, toluene, and C8-C10 aromatics is 0.69 ppb in NYC and 0.43 ppb in Boulder. The ALPACA median mixing ratio for this sum is 8.66 ppb, which is 12–20 times higher than the other two locations. In addition, the contribution of aromatics to the TVOC mixing ratio is just 5% in NYC and 10% in Boulder, but 43% in Fairbanks. For ethanol, the medians are 7.54 ppb in NYC and 2.01 ppb in Boulder with Fairbanks falling in the middle at 4.39 ppb. In contrast to the aromatics, ethanol is just 22% of the TVOCs in Fairbanks, but 57% and 45% of the TVOCs in NYC and Boulder, respectively. In summary, Fairbanks features a fundamentally different atmospheric composition when compared to NYC and Boulder, with the highest total VOCs and a much greater contribution to the total from aromatics, but a smaller contribution to the total from ethanol, possibly indicating a smaller contribution from personal care products. This may imply that the discretionary use of VCPs may also be lower in nations/areas with lower per capita incomes.

Four measured furanoids were present at the house at low campaign-average mixing ratios (Table S2 in Supporting Information S2): furan (0.093 ± 0.072 ppb), methyl furan (0.10 ± 0.08 ppb), furfural (0.089 ± 0.075 ppb), and methyl furfural (0.050 ± 0.034 ppb). These species were highly correlated with each other (Table S1 in Supporting Information S2, Figure 4d) and peaked in abundance at night (Figure 3a), consistent with nearby RWC home heating (Gilman et al., 2015) with minimal transport times to the measurement site. They would be expected to react quickly with NO_3, especially at night (Figure 2d; Decker et al., 2021), contributing to their low average abundance. Other, mostly longer-lived VOCs commonly reported at molar ratios to CO of 0.005–0.02 in fresh BB emissions in the literature were present at average mixing ratios, consistent with assuming that BB accounted for roughly 50%–70% of each of these VOCs (vide infra) and that BB also accounted for 30–150 ppb of the 540 ppb average total CO (i.e., ∼5%–25% of CO from BB). These VOCs include formaldehyde (1.39 ± 0.89 ppb), acetaldehyde (1.33 ± 1.07 ppb), formic acid (0.96 ± 0.52 ppb), acetone (1.13 ± 0.62 ppb), acetic acid (1.30 ± 0.66 ppb), and hydroxyacetone (1.32 ± 0.69 ppb) (Table S2 in Supporting Information S2). Acetonitrile is often used with CO as a marker for generic open BB (i.e., "vegetation fires") but is less useful for identifying air masses impacted by RWC due to the low N content of firewood (Akagi et al., 2011; Coggon et al., 2016; Traviss et al., 2024). Acetonitrile plotted versus CO had a slope of 0.031 ppb ppm^{-1} and r^2 of 0.27. The slope is much lower than typical urban values (0.26 ppb ppm^{-1}) impacted by acetonitrile use as a solvent and other influences (Huangfu et al., 2021). In contrast, the average acetonitrile/CO ratio for open BB is near 2.0 ppb ppm^{-1} (Permar et al., 2021), and typical acetonitrile/CO ratios above which a BB influence is assumed, 2.00–2.35 ppb ppm^{-1} (e.g., Huangfu et al., 2021; Juncosa Calahorrano et al., 2021), are ∼70 times higher than the observed ALPACA average. Furanoids, which are normally associated with BB, also correlated poorly with acetonitrile (Table S1 in Supporting Information S2). These observations nevertheless leave room for a significant contribution from burning firewood due to its low N content noted above. Finally, a peak at protonated *m/z* 69.070 (C_5H_8 neutral formula) calibrated as "isoprene" averaged 0.85 ppb but is likely a fragment of higher masses (Coggon et al., 2024; Hu et al., 2015) as this peak correlated best with aromatics and the biogenic influence is negligible due to low temperatures (Table S2 in Supporting Information S2).

3.2. Overview of Particulate Matter Observations

We begin by comparing the degree of fine particulate matter pollution at the house to other sites in Fairbanks (Table S2 in Supporting Information S2). The campaign average of the hourly average TNRM (the sum of the AMS-measured species) was 13.59 ± 12.69 μg m^{-3} (range 0.23–86.15 μg m^{-3}). The campaign average of the hourly average BC was 1.31 ± 1.25 μg m^{-3} (range 0.00–6.47 μg m^{-3}). $PM_{1.0}$ was estimated as the sum of TNRM and BC and the campaign average of the hourly average $PM_{1.0}$ was 14.96 ± 13.99 μg m^{-3} (range 0.23–90.90 μg m^{-3}). The nearest regulatory site at A-street measures 24-hr average $PM_{2.5}$ gravimetrically and reported 11.4 ± 6.35 μg m^{-3} averaged across the campaign (19 January to 25 February). However, the A-street site was not operational for 12 of those days, mostly during the most heavily polluted and coldest 9 days. A stricter comparison of the regulatory and ALPACA data is possible, but the house data could be more representative of Fairbanks than A-street during the campaign due to the large data gaps at the latter site. Table S2 in Supporting Information S2 also shows the campaign average for comparable PM species at CTC: BC averaged 1.60 ± 1.43 μg m^{-3} and TNRM averaged 8.3 ± 9.3 μg m^{-3} for a $PM_{1.0}$ of 9.6 ± 10.3 μg m^{-3}.

PM/CO ratios can be used to flag or indicate BB smoke impacts (Jaffe et al., 2022; McClure & Jaffe, 2018; Selimovic et al., 2020). In the Northwestern United States, fresh wildfire smoke injected in the summer atmosphere at high elevation (e.g., ∼5 km) and near zero degrees Celsius typically has $PM_{1.0}$/CO mass ratios near 0.25 g g^{-1}. If the smoke descends and impacts urban areas, dilution and warming lower the PM/CO mass ratio to ∼0.125 g g^{-1} (Pagonis et al., 2023). The same urban areas have much lower PM/CO mass ratios in the range of 0.01–0.05 g g^{-1} when there are no, or only minimal, smoke impacts (Jaffe et al., 2022; McClure & Jaffe, 2018; Selimovic et al., 2020). Fresh woodstove emissions at room temperature have PM/CO ratios near 0.17 g g^{-1} (Traviss et al., 2024). At the house, outdoor $PM_{1.0}$ plotted against CO for the ALPACA campaign has a slope of 0.02 g g^{-1} and r^2 of 0.82. This is similar to the ratios observed in smoke-free urban areas. At the house, only a few hourly $PM_{1.0}$/CO ratios are above 0.05 g g^{-1}. Thus, the CO/CO_2, VOC/CO, and the $PM_{1.0}$/CO ratios at the house in winter are similar to commonly observed values associated with low or no smoke impacts in small cities.

A key feature of the chemical composition of the PM during winter in Fairbanks is high concentrations of sulfate (e.g., Simpson et al., 2020, 2024; Wang & Hopke, 2014). As noted earlier, from 2006 to 2010 ultralow sulfur diesel (ULSD, 15 ppm S) was phased in for vehicles and noncoal power plants leaving three main sulfur-rich

fuels. Jet fuel is the main regional sulfur source (JP8 with 900 ppm S is used at both Fairbanks international and military airports), but, as with power plants (Brett et al., 2025), the emissions are not thought to heavily influence surface air quality. Firewood (~100 ppm S, Traviss et al., 2024) does not burn efficiently enough to convert as much of the fuel S to SO_2 (or fuel N to NO_x) compared to highly efficient fossil fuel combustion (e.g., Dai et al., 2019; Roberts et al., 2020; Tab. 3; Fig. 12 in Yokelson et al., 1996). At the time of the ALPACA campaign, the typical mix of number 1 and 2 heating oil that was in use is estimated to have ~1,800 ppm S and only #1 oil (900 ppm S) was allowed for refilling tanks starting 1 September 2022 (after ALPACA). In addition, the use of natural gas (17 ppm S) for heating is encouraged (https://www.interiorgas.com/our-mission/). The September 2022 decrease in the heating oil sulfur standard has already resulted in significantly lower SO_2 mixing ratios at the NCore site as noted earlier.

Evolving regulations and the different neighborhood preferences for heating likely drive the site-to-site variability observed in both the particulate sulfate content and the relative ranking of major PM sources at each site. A winter 2020 study provided some particulate composition data at two sites relying mainly on commercial and residential distillate oil combustion for space heating (NCore and A-street) and one site relatively more impacted by RWC (Hurst) (Simpson et al., 2020). The $SO_4/PM_{2.5}$ mass ratios (based on IC SO_4) at these 2020 sites were 0.191, 0.164, and 0.084, respectively, and a mass ratio of 0.20 (based on AMS SO_4 and $PM_{1.0}$) was observed at the ALPACA house. At CTC, the AMS-based $SO_4/PM_{1.0}$ mass ratio was about 18% lower than at the house at 0.165. An aerosol chemical speciation monitor operating with a $PM_{2.5}$ cutoff during ALPACA and for two previous winters at NCore measured a 3-winter average SO_4/OA ratio near 0.17 (Robinson et al., 2024), which is 41% lower than the value measured with the AMS at nearby CTC (0.29) during ALPACA and 50% lower than the AMS-based house site average ratio of 0.34 during ALPACA. The IC-based NH_4/SO_4 winter 2020 mass ratios were 0.41, 0.38, and 0.036, respectively, and during ALPACA, 0.28 was measured at the house site and 0.26 at CTC using AMS. The house and CTC NH_4/SO_4 ratios would be higher if the AMS SO_4 is too high due to measurement interference from organic sulfur. Overall, these comparisons show that the house and CTC sites resemble the areas mainly burning oil rather than the areas relying more on wood burning. However, we reiterate that the greater Fairbanks area as a whole (including North Pole which is out of attainment for $PM_{2.5}$) likely uses more wood and possibly natural gas for indoor heating than the ALPACA house and CTC sites.

The largest component of the winter 2022 fine PM at the house during ALPACA was OA (8.7 ± 8.6 μg m^{-3} with a range of 0.11–70 μg m^{-3}), comprising 64% of TNRM or 58% of $PM_{1.0}$. It is of interest to compare the abundance of gas-phase aromatic VOCs, which are potential precursors for secondary OA (SOA) to the condensed phase OA. The ratio based on campaign average abundances is 11.98 ppb aromatics/8.71 μg m^{-3} OA. We can convert this ratio to an estimated mass ratio assuming an average molar mass of ~100 g mol^{-1} for the aromatic VOCs. With this assumption, 1 ppb of aromatics is equivalent to 4.46 μg m^{-3} of aromatics (273 K, 1 atm) and 11.98 ppb of aromatics corresponds to 53.4 μg m^{-3} of aromatics. Thus, without allowing for other precursors or SOA yields <1, the mass of potential gas-phase OA precursors is at least ~6 times the mass of OA, indicating only a modest degree of aging, consistent with the low SOR and pNO_3/NO_x ratios mentioned above. An analogous estimate considering the campaign average TVOC of 32.7 ppb suggests that the reactive organic carbon (ROC, we exclude methane, which is long-lived per Heald et al., 2020) at the house during winter is heavily weighted toward the gas phase. Figure 5 shows a rigorous calculation of the observed ALPACA campaign-total mass of reactive organic carbon present in the gas phase (based on the PTR-TOF-MS and CRDS HCHO) versus the condensed phase (based on the AMS) at the house. Most of the gas-phase nonmethane alkanes were not measured during ALPACA, but they accounted for ~25% of the total ROC in urban Southern California during CalNex (Heald et al., 2020). Assuming the same gas-phase alkane fraction of ROC for ALPACA would imply that OA accounted for only 6% of ROC, which is similar to the OA fraction of ROC of 5% for both urban and biogenic summertime environments reported by Heald et al. (2020), but about 10 times lower than observed for fresh BB emissions, especially at low temperatures (Gkatzelis et al., 2024; May et al., 2013; Pagonis et al., 2023). Assuming alkanes account for 25% of gas phase ROC in Fairbanks also suggests that aromatics and alcohols together contributed ~55% of gas phase ROC in Fairbanks during ALPACA. A combined contribution this large of aromatics and alcohols to ROC has not been previously observed in an urban environment to our knowledge, highlighting the unusual emissions profile in Fairbanks during wintertime.

Figure 3d shows the diel cycles for TNRM and BC. Both TNRM and BC decrease slowly in the early morning until a rise starts at 05:00. Both peak at 08:00 and then subside to a midday low at 11:00. After that, TNRM rises faster than BC, probably due to secondary production and both reach their daily maximum at 19:00. After 19:00,

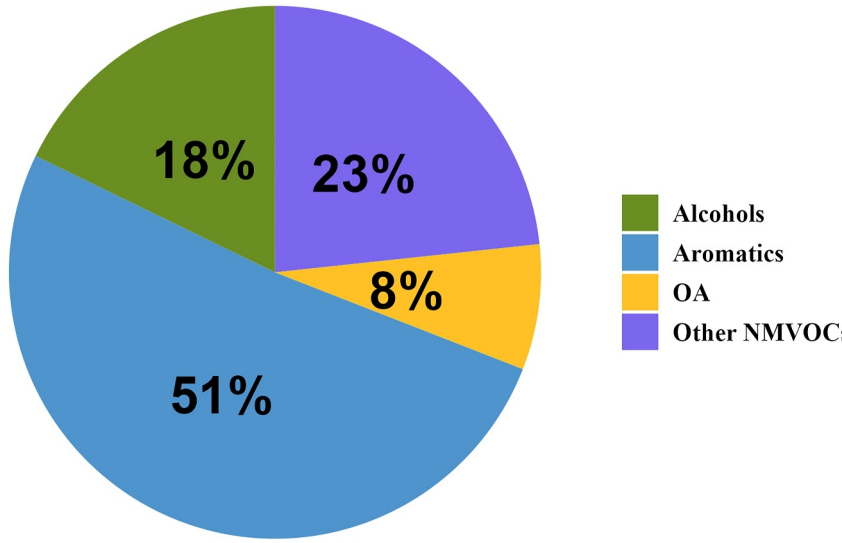

Figure 5. Mass distribution of measured reactive organic carbon at the house site in Fairbanks during ALPACA. This distribution is derived from the campaign average total ROC, totaling 113.78 μg m^{-3}. ROCs for gas-phase species were calculated using ambient temperature and pressure measured at CTC. CO, CO_2, and CH_4 were excluded from this analysis due to their long atmospheric lifetimes. The "OA" is organic aerosol. The "Other NMVOCs" category would be larger if we included unmeasured alkanes and the VOCs that were observed by PTR-TOF-MS, but not quantified in this work (about 6% of the VOC raw signal on the PTR-TOF-MS).

both decrease slowly unlike many VOCs associated with BB, which peak near midnight (Figure 3a). The morning peak and larger afternoon peak in both TNRM and BC imply that traffic and secondary formation are important PM sources, but there is significant potential for other sources to contribute given the high baseline.

3.3. Semiquantitative Source Apportionment Based on PMF

3.3.1. Factor Profiles, Assignment to Sources, and Source Contributions

In Section 2, we summarized the PMF5.0 model setup and sensitivity tests. Here, we present and discuss the PMF results starting with the key factor characteristics that supported our assignment of factors to specific sources for data set #1. These assignment protocols almost always applied equally well to the PMF factors based on data sets #2 and #3. We also summarize the PMF-calculated contributions of each source to the total fit concentrations of various key pollutants. For reference throughout the discussion, Table S4 in Supporting Information S2 presents the full factor concentration profiles, the factor assignment to sources (e.g., traffic, heating oil combustion, and biomass burning), and the source contributions to the total fit signal for each pollutant in the input file for the 6-factor solution.

One easily assigned factor that occurred in all the PMF experiments accounted for ~98% of O_3. The time series of this factor's contribution to the fit for each sample matched the O_3 mixing ratio time series and this factor's contribution to the total fit for all species other than O_3 was very low except for modest contributions to acetonitrile, CO_2, and CH_4. We have associated this factor with meteorology-driven surface impacts of regional background air (short name "O_3-background" or just "O_3"). Another recurring factor in all the PMF runs had ratios for NO_2/NO, pNO_3/NO_x, and OA/aromatics that were much higher than for any factor assigned to a fresh source (Table S4 in Supporting Information S2). This factor made major contributions to total NO_2, pNO_3, NH_4, and Chl and significant contributions to total OA and SO_4, but no contribution to total NO. We have assigned this factor to pollution generated mostly by local traffic and possibly some heating oil combustion that has aged in place for several hours (i.e., long enough to convert NO to NO_2) rather than aging along with recirculation, which could add O_3. We named this factor "slightly aged" or "aged" for short.

A third factor found in all our PMF solutions had a profile with the highest ratio of SO_4 to OA. Since heating oil is the most S-rich fuel (~1,800 ppm S during ALPACA) thought to impact the surface, it is a good candidate for this factor's assignment. Coal-fired power plants and aviation emissions are mainly injected at altitude and only

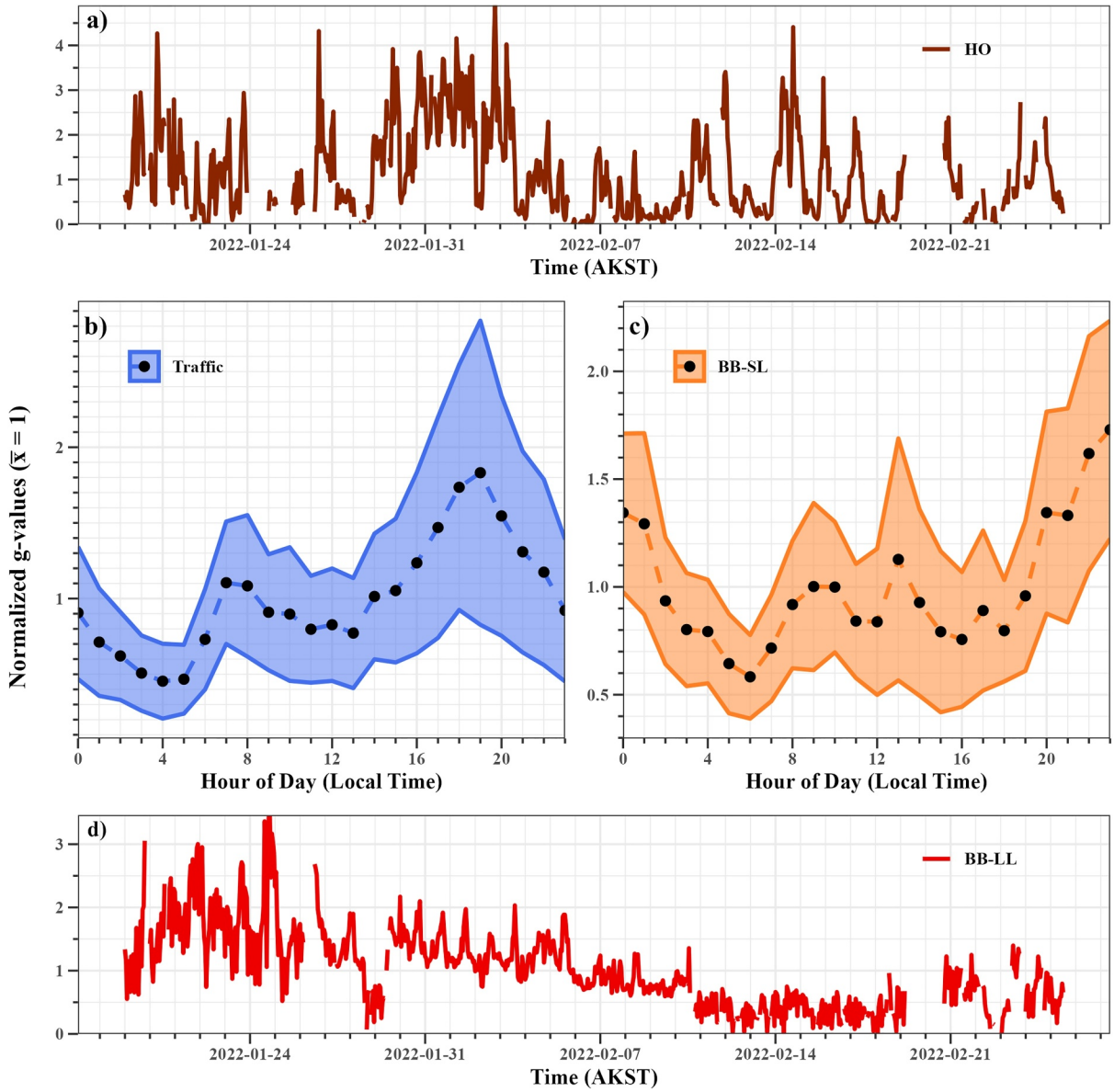

Figure 6. Selected properties of factors in the 6-factor PMF solution. The variation in a factor's coefficients should be consistent with the factor assignment to a source. (a) The coefficient for the fixed factor concentration profile assigned to heating oil combustion (HO) is shown versus time across the ALPACA campaign. Note the sustained high values during the cold event centered around 1 February 2022. (b) The diel cycle of the coefficients for the factor assigned to traffic. Note the rush hour peaks similar to those in the diel cycles for traffic emissions in Figures 3b and 3c. (c) The diel cycle of the coefficients for the factor assigned to short-lived VOCs from nearby home heating with wood (BB-SL). The factor's coefficients peak at night, similar to the furanoids shown in Figure 3a, and as would be expected if there are minimal transport times between the source and the measurement location. (d) The coefficient for the factor assigned to longer-lived VOCs from regional home heating with wood (BB-LL) is shown versus time across the ALPACA campaign. The coefficients are larger during January when regional home heating needs are likely larger.

weakly impact the surface in Fairbanks during inversions (Brett et al., 2025). Four additional pieces of evidence support this factor's assignment to heating oil combustion. (a) The factor's contribution to the fit for each sample peaked during the coldest ambient temperatures (Figure 6a). (b) We found that a measured particulate species source profile for heating oil combustion intended to represent Fairbanks conditions and recommended by ADEC correlated highly with this PMF factor's profile ($r^2 = 0.98$, Ward, 2013; Figure S3a in Supporting Information S1). The comparison is excellent, but there are some caveats. While the fuel for the ADEC profile was from Fairbanks, the ADEC profile sulfate measurement was by IC and potentially not completely equivalent to the AMS sulfate we based our PMF on. We also do not know the temperature of the dilution air or the age/condition of the furnace used in the circa 2012 ADEC-supported tests and how well it represented furnaces in use in Fairbanks in winter

2022. The furnace in the house was likely installed during construction in 1985 or replaced before 2000, and the neighborhood was likely dominated by similarly old oil furnaces. (c) We acquired one sample of the furnace exhaust while running at high efficiency (CO/CO_2 = 0.000145, Table S3 in Supporting Information S2) and nevertheless observed a very high $PM_{2.5}$/CO ratio (403 μg m^{-3} ppm^{-1}; based on a preliminary estimate of $PM_{2.5}$). This high $PM_{2.5}$/CO ratio indicates a high emission factor for $PM_{2.5}$, especially during less efficient combustion. This is consistent with previous observations of large SO_3 and primary sulfate emissions from high-temperature combustion of diesel heating oil and other high-S diesel fuels, especially in older devices (Dai et al., 2019; Office of Research and Development, 1978). (d) Our one sample of the house site furnace VOC emissions (Table S3 in Supporting Information S2) agreed well with this PMF factor profile except our measured HCHO was lower than in the PMF profile. In summary, strong evidence supports the assignment of this factor to heating oil combustion (HO).

A fourth factor made the largest contribution to the campaign total fit for aromatics, CO, NO, and NO_x; all species were associated with "traffic" via their diel cycles. This factor was also the largest source of BC when BC was added to data set #2 Section 3.3.3. The diel cycle for this factor's coefficients had sharp rush hour peaks (Figure 6b) and the factor's coefficients peaked during the warm event.

Finally, two factors with high relative concentrations of VOCs traditionally associated with biomass burning (BB) in their profiles were consistently generated by our PMF model runs. One of these factor's profile always had the largest concentration values for furan, substituted furans (furanoids), and the furan oxidation product maleic anhydride, which are all short-lived due to rapid reactions with OH or NO_3. This factor always made the largest contributions to the campaign total fit for the furanoids. The diel cycle of the factor's coefficients for the fit to each sample peaked at midnight (Figure 6c). This factor can be associated with fresh BB, likely RWC at nearby homes and our short name is "BB-SL." The other BB factor profile was dominated by longer-lived or secondary BBVOCs ("BB-LL", e.g., methanol, acetic and formic acid, etc.). This factor always accounted for >90% of the campaign total fit for formic acid, a known major secondary VOC in BB plumes (Akagi et al., 2012; Permar et al., 2023) and is likely representing regional wood burning at North Pole etc. This factor's coefficients for the fit to each sample showed an overall decrease from January to February (Figure 6d). The average of these two PMF BB factor's particulate species profiles correlated well with a measured "local" RWC profile that was recommended by ADEC and also performed the best in the CMB-based source apportionment of Ward (2013) (Figure S3b in Supporting Information S1, r^2 = 0.99), but there are not a lot of intermediate values to challenge the regression. The splitting of BBVOCs into two factor profiles similar to ours has a strong precedent in the recent BB literature. Sekimoto et al. (2018) found that PMF could model the time series of over 100 BBVOCs measured in fresh lab-simulated wildfire smoke with just two factors that they attributed to low- and high-temperature pyrolysis, respectively. Later, Roberts et al. (2020) were able to fit the same BBVOC measurements plus the simultaneously measured, inorganic, N-containing gases using the two Sekimoto factors plus a third "combustion" factor. Sekimoto et al. (2023) then showed that their two lab-measured factors for wildfire smoke plus an aging factor fit the BBVOCs measured in aircraft sampling of wildfire smoke up to 8 hr old. In this Fairbanks study, the BBVOCs are from the combustion of wood only (RWC) and embedded in a multiage complex urban mixture. Remarkably, with a handful of exceptions, the BBVOCs that we attribute to our short-lived factor were assigned to the low-temperature factor by Sekimoto et al. (2018) and our long-lived BBVOCs were assigned to the high-temperature factor by Sekimoto et al. (2018) as shown in Table S4 in Supporting Information S2. Visual representations of the time series, diels, and contributions of individual species to each factor are shown in Figures S4 and S5 in Supporting Information S1.

Having assigned sources to all the factors in the 6-factor solution for data set #1, we can now focus on the contribution of each source to the campaign total fit amount of any species in the model. The campaign total contributions of each source for all the species included in the model are shown in Table S4 in Supporting Information S2 and selected results are illustrated in Figure 7.

In the ensuing discussion, we summarize the source contributions to a few key species that are of widespread interest as pollutants: PM, CO, SO_4, NO_x, HCHO etc. In most cases, we show the source contribution from the model run with the lowest Q value (the best or "central" estimate), followed by the range of possible source contributions constrained by DISP analysis allowing a small increase in Q of no more than 4. Recall lower values of Q, the objective function, correspond to better fits. The range in source contributions from an allowed change in

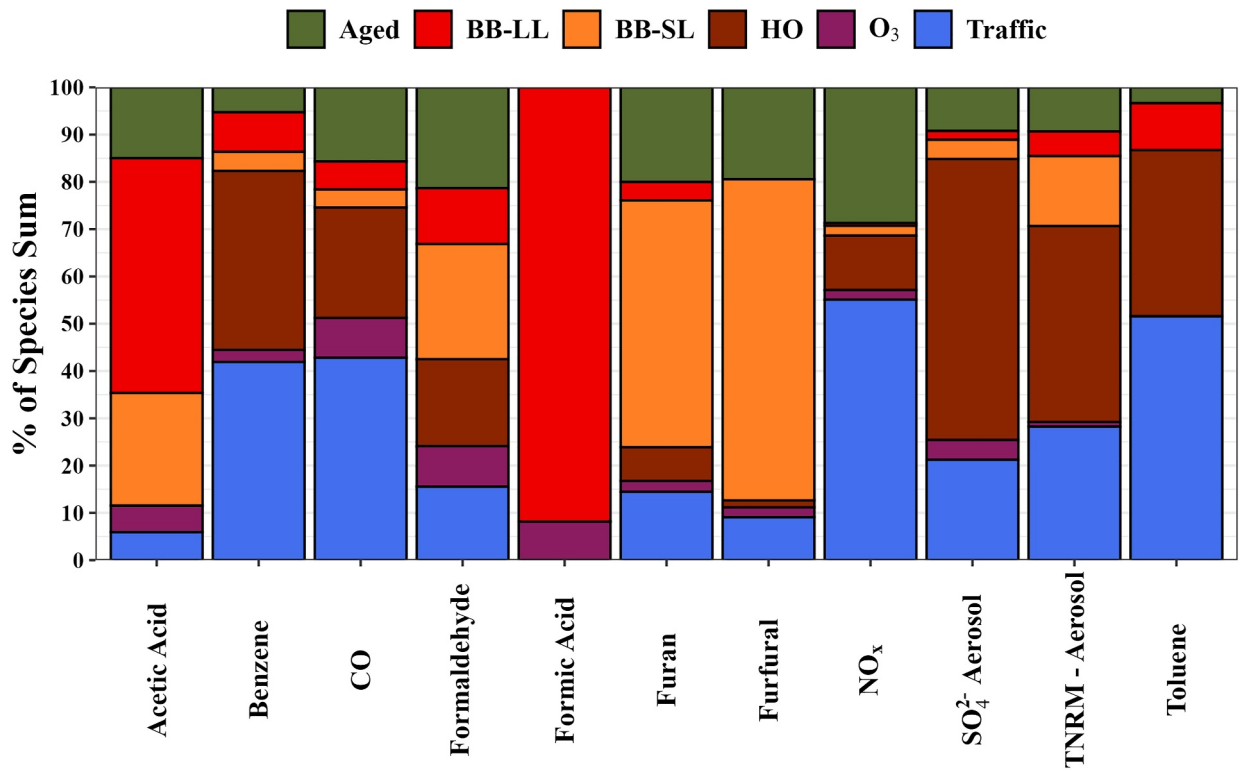

Figure 7. Percent contributions of PMF factors to the total fit concentrations of key particle and gas phase air pollutants.

Q of four is roughly equivalent to a 95% confidence interval. If only one number is shown (to improve readability), it is the best/central estimate.

PM is currently the dominant air quality concern in the Fairbanks area. The apportionment of PM sources based on the 6-factor solution for the data set #1 TNRM is heating oil 41% (37%–47%), traffic 28% (25%–32%), the combined BB factors 20% (15%–27%), aged pollution 9% (6%–12%), and regional background ("O_3") 1% (0.5%–1.8%). The full breakout in Table S4 in Supporting Information S2 shows that SO_4 and NH_4 had dominant contributions from HO and traffic (in decreasing order). OA had significant contributions from traffic, HO, and BB. Chl and pNO_3 had similar contributions from HO, traffic, aged air, and BB.

From a regulatory standpoint, if we assign the PMF factor dominant in sulfate to heating oil combustion (as supported earlier), then HO accounts for about 40% of TNRM, leaving traffic and BB to divide most of the rest. This source apportionment is specifically for the house neighborhood and could be biased compared to a more regional source attribution, for example, if the house and the surrounding neighborhood rely relatively more (or less) on oil heat than other areas of Fairbanks. In addition, the most viable strategy to reduce PM levels does not necessarily have to target the largest PM source. Nevertheless, the house site experiences high pollution events (Figure 1c) and these PMF results support the recent lowering of the heating oil sulfur standard as one measure to lower PM in Fairbanks.

Fairbanks has extremely high concentrations of NO_x in winter (ALPACA campaign average at the house is 53 ppbv, Table S2 in Supporting Information S2). Traffic and slightly aged pollution mostly from traffic were the main sources of NO_x in our 6-factor PMF solution for data set #1, contributing 55% (53%–58%) and 28% (26%–34%), respectively. Breaking out NO and NO_2 separately showed traffic producing 86% (83%–90%) and 5% (4%–7%) of NO and NO_2, respectively, while the aged factor contributed 0% (0%–0.3%) and 66% (61%–76%) of NO and NO_2, respectively.

Traffic was also the main source of CO (43%, 41%–45%), followed by heating oil (23%, 19%–25%), aged pollution (16%, 14%–19%), and BB (10%, 8%–13%). Traffic was the main source of the dominant aromatic VOCs (Section 3.1), which are important SOA precursors ranging from 42% (40%–44%) for benzene to 52% (49%–55%)

for toluene. Heating oil combustion was the second largest source of aromatic VOCs. The sum of the aromatic VOCs as a percent of the profile divided by the OA as a percent of the profile was 6.1 times larger for fresh traffic than for aged pollution (Table S2 in Supporting Information S2), consistent with the expectation that aging converts aromatic VOCs to OA. The toluene/benzene ratio for the aged factor profile (1.44) was about half the ratio in the fresh traffic profile (2.78), consistent with the slope of the regression (2.89) in Figure 4 and the larger OH rate constant for toluene. Traffic and aged pollution were the two main sources of methanol and ethanol, which are relatively long-lived VOCs and present at high concentrations in Fairbanks (Section 3.1).

The combined BB factors were dominant for many other VOCs such as formic acid (92%, 80%–97%), acetic acid (73%, 65%–89%), hydroxyacetone (69%, 61%–83%), furfural (68%, 60%–74%), methyl furfural (57%, 50%–76%), furan (56%, 50%–74%), and methyl furan (55%, 49%–73%). "Isoprene" was 48% (46%–52%) from heating oil and most correlated with aromatics, again supporting that C_5H_8 was a fragment signal during winter. Several VOCs had similar contributions from many sources. For example, HCHO sources were attributed as local ("SL") BB (24%), slightly aged pollution (21%), heating oil (18%), traffic (16%), regional ("LL") BB (12%), and regional background (9%) (Table S4 in Supporting Information S2).

3.3.2. Comparison to Previous Work and Other ALPACA Findings

The source apportionment from the above PMF on data set #1 can be compared to previous work in Fairbanks and other results from ALPACA both of which are dominated by source apportionments for PM. Thus, we focus on our 6-factor data set #1 solution central estimate that BB accounts for ~20% (15%–27%) of TNRM at the house site. (Note that doubling the uncertainty assigned to the VOCs measured on inlet A relative to the inlet B species uncertainties *decreased* the modeled BB-PM contribution to 15%.) Some previous studies have identified BB (herein essentially the same as RWC in Fairbanks winter) as the main source of fine PM at various Fairbanks locations. For example, Kotchenruther (2016) using PMF estimated that primary (39.9%) plus aged (12.8%) woodsmoke accounted for 51.8% of December-January Fairbanks $PM_{2.5}$ at NCore from 2009 to 2014. Other studies have found that either BB or heating oil could be the largest single winter $PM_{2.5}$ source depending on the location (Simpson et al., 2020; Tab. 14 in Ward, 2013), but that BB still contributed 31%–36% of $PM_{2.5}$ at oil-dominated sites as determined by CMB (Tab. 14 in Ward, 2013). Busby et al. (2016) used the same filter samples collected from 2008 to 2011 as Ward (2013), but analyzed them with additional techniques, comparing and evaluating radiocarbon (^{14}C), CMB, and levoglucosan-based source apportionment methods in Fairbanks. Busby et al. (2016) concluded that CMB overestimated woodsmoke and that the levoglucosan-based approach was the most reliable for wintertime in Fairbanks from 2008 to 2011. Using the levoglucosan approach, the 3-winter average percentage of $PM_{2.5}$ attributable to woodsmoke was 26%–35% at the State Building (close to CTC), 20%–30% at Peger Road, and 42%–62% at North Pole. Wang and Hopke (2014) performed receptor modeling using PMF5.0 based on filter measurements of elements, ions, EC, and OC collected from 2005 to 2012 at the State Building. They found that woodsmoke accounted for 39.6% of $PM_{2.5}$ in winter. Their time series of factor contributions to the sample fits for IC sulfate, diesel, and nitrate also peaked in winter and together these sources accounted for 48% of $PM_{2.5}$ in winter. One recent PMF-based study using filter data collected at NCore from 2013 to 2019 (Ye & Wang, 2020) found a BB contribution to wintertime $PM_{2.5}$ (17.3 ± 1.3%, similar to the 6-factor central estimate of 20% in this work) and a significant winter $PM_{2.5}$ contribution from traffic (21%). The largest wintertime $PM_{2.5}$ source found in Ye and Wang (2020) was S-containing fuel combustion (43.7%, measured by IC). Our findings agree best with the reanalysis by Busby et al. (2016) and the recent study by Ye and Wang (2020).

During ALPACA, Ijaz et al. (2024) collected HR-AMS data at the nearby CTC site. Their PMF analysis of the OA found that it was 29% BBOA and 19% OOA (Fig. 6b in Ijaz et al., 2024). If we make the upper limit assumption that all the OOA mass is aged BB emissions (vide infra), then we get a maximum BB contribution to OA of 48%. Since OA was 68% of TNRM at CTC (Ijaz et al., 2024; Table S1 in Supporting Information S2), it follows that the upper limit BB contribution to TNRM would be 33%. This is about 20% larger than the high end estimated at the house by the 6-factor PMF and not a large difference given the uncertainties in both the measurements and analyses and site-to-site variability. Evidence that the OOA mass in the OA breakout at CTC is not all from BB includes the observation that the BB markers *m/z* 60 and 73 accounted for only a few tenths of a percent of the total OOA signal (Fig. S10 in Ijaz et al., 2024). Further, PMF applied to the TNRM at CTC isolated a single OOA factor that was more than 40% sulfate and almost 60% inorganic (Fig. S15 in Ijaz et al., 2024). Thus, the

assumption that all the OOA mass is from RWC emissions in the TNRM breakout seems less justified than for the OA breakout. At temperatures somewhat similar to ALPACA (~0°C at high altitude in the Western United States), recent BB campaigns measured an average BBOA/BBPM$_{1.0}$ ratio of 0.923 (Gkatzelis et al., 2024; Liu et al., 2017). This should be a low estimate of the BBOA/BBPM$_{1.0}$ ratio for RWC because the nitrogen and sulfur content in wood is about six to four times lower, respectively, than in the biomass that burns in a typical wildfire (Selimovic et al., 2018; Traviss et al., 2024). Such a low inorganic content in BBPM is consistent with a large non-BB contribution to the OOA at CTC in the TNRM breakout of Ijaz et al. (2024) and also justifies the fact that we have ignored any small BB contribution to the inorganic mass at CTC. To facilitate comparisons with source apportionments for PM$_{2.5}$, we note that the TNRM/PM$_{1.0}$ ratio at CTC was 84% making 27% an upper limit for the BB contribution to PM$_{1.0}$ or PM$_{2.5}$ if we ignore a possible small contribution of BB to the total BC. This agrees well with the RWC contributions to PM$_{2.5}$ in Fairbanks estimated by Busby et al. (2016) and is consistent with our PMF-based source apportionment at the nearby house site.

Positive values of Delta-C (the BC measured at 370 nm minus the BC measured at 880 nm by an aethalometer) have been shown to correlate with levoglucosan and serve as an indicator of RWC (Wang et al., 2011). Comparing their Delta-C values with organic marker species, Wang et al. (2011) reported an annual average Delta-C concentration of 0.110 μg m^{-3} for 2010 to 2011 in Rochester, NY and a corresponding woodsmoke concentration of 0.72 μg m^{-3}, while Wang et al. (2012) found that a 4-year (2007–2010) average Delta-C value of 0.141 μg m^{-3} was associated with a woodsmoke concentration of 0.82 μg m^{-3}. These studies are consistent with a woodsmoke concentration to Delta-C mass ratio of 6.2 ± 0.49. If this ratio applies to Fairbanks, multiplying it times the ALPACA house site average Delta-C of ~0.5 μg m^{-3} suggests an average woodsmoke concentration of about 3.1 μg m^{-3}, which is ~23% of the average house site TNRM of 13.59 μg m^{-3} and ~21% of the average house PM$_{1.0}$ of 14.96 μg m^{-3} (Table S2 in Supporting Information S2). These percentages agree well with the 6-factor PMF-based estimate that BB accounts for ~20% of TNRM at the house.

Finally, a concern with our 6-factor, data set #1 PMF results was that our unfit residual TNRM (mostly at spikes) was about 15%–20% of the total measured TNRM and this residual, in theory, could be added to the contribution for BB or some other source. However, we note that the speciation of the residual TNRM was almost identical to the speciation of the fit TNRM (slope = 1, $r^2 = 0.98$), consistent with the unfit TNRM being a mix similar to the fit TNRM. Overall, the remaining uncertainty/ambiguity between studies in the fine PM source attribution after using data set #1 motivated us to pursue additional PMF analyses based on alternative input data sets.

3.3.3. Investigating PMF Precision and Dependence on Input Data

To determine if different or better PMF solutions might result from other reasonable options for the input data, our first step was to create data set #2, which included all the outdoor data from both inlet systems even if they were out of phase. We also added BC, PM$_{1.0}$ (calculated as TNRM + BC), naphthalene, and a few other VOCs to this input data set. With the added data, 6-factor solutions were unsatisfactory. In all the 6-factor PMF model runs with input data set #2 the residuals increased, CO and PM$_{1.0}$ from BB were <5% and about 18%, respectively; traffic became the main PM$_{1.0}$ source at ~38%, and the BC contribution of heating oil was zero. Selecting 7 factors resulted in smaller residuals, an additional heating oil factor that, when averaged with the other heating oil factor, restored good agreement between the PMF HO profile and the ADEC local HO profile (r^2 0.98, Figure S1c in Supporting Information S1). Heating oil combustion was also restored as the main PM$_{1.0}$ source at 54%. Traffic and HO were the main BC sources accounting for 56% and 28%, respectively. However, this solution attributed just 12.5% of PM$_{1.0}$ and 2% of CO to BB, which drew us further from "agreement" with the assumption that BB is the main or codominant PM source. Increasing to 8 factors further decreased residuals and split the traffic into two factors: one dominated by NO and BC, and the other by CO and aromatics, potentially related to diesel and gasoline respectively. Heating oil was the main PM$_{1.0}$ source at 44%–62% and BB accounted for 11%–13% of PM$_{1.0}$ and 4%–6% of CO across several model runs.

The 9-factor result with data set #2 and the warm event truncated (23–25 February) was particularly interesting (Table S5 in Supporting Information S2). Increasing to nine factors resulted in traffic accounting for three factors dominated individually by CO and aromatics, BC, or NO. Evidence exists for naming a high-S factor ("factor six"), which accounted for 45 (39–50)% of PM$_{1.0}$, as either HO or as secondary aerosol. For instance, the average of factor 6 with factor 3, which we could confidently assign to HO, correlated well with the ADEC local HO

profile (r^2 = 0.96, Figure S1d in Supporting Information S1). Factor 6 alone and factor 3 alone also both correlated well with the ADEC local HO profile. The factor 6 (and factor 3) contributions to the fits for each sample peaked during the cold event. The age of the house furnace makes high PM emissions more likely (Office of Research and Development, 1978). In addition, Yang et al. (2024) estimated an average air-mass residence time at the house site of only 2 hr. However, the case to name factor 6 as slightly aged aerosol is also strong. Brett et al. (2025) suggest air mass ages during ALPACA could reach 2 days. The diel cycle of the factor 6 contributions to the samples has a small peak in the afternoon, consistent with TNRM starting to rise before BC in these species' diel profiles (Figure 3d). When normalized as a percent of the profile total, all the AMS species except chloride are higher and most of the secondary-PM precursor gases are lower in the normalized factor 6 profile than in the normalized factor 3 profile. In addition, chemical aging not dependent on photochemistry is known to be important in Fairbanks (Campbell et al., 2024; Dingilian et al., 2024; Mao et al., 2024; Moon et al., 2024) and changes to particle chemistry and the production of particles with mass from more than one combustion source are inevitable due to evaporation, condensation, and coagulation, which is proportional to the number concentration (Akagi et al., 2012; Carrico et al., 2016; Hobbs et al., 2003). Finally, filter analyses discussed further below confirm that there were significant amounts of secondary sulfur species during ALPACA.

A precise, well-defined determination of the relative contributions of primary and secondary species typically requires measurements of a suite of species that can only be created by secondary processes, isotopic analyses, and/or specialized sampling such as pseudo-Lagrangian plume sampling (e.g., Akagi et al., 2012) of species that could be deemed primary or secondary depending on a somewhat arbitrary selection of an age at which further change is defined as "secondary." For example, partitioning is impacted by dilution and there are significant and variable SO_3 emissions from furnaces that can react with water to form SO_4 on very fast timescales. Many other important secondary pathways can quickly affect the SO_4 and non-SO_4 content of particles involving not just available SO_2 and OH or SO_3 and water but also NH_3, NO_2, H_2O_2, O_3, transition metals, aldehydes etc. (Finlayson-Pitts & Pitts Jr, 2000; Moon et al., 2024). SO_2 from HO combustion can be coemitted with large amounts of NH_3; the national average NH_3/SO_2 molar emission ratio for HO combustion is 0.5 according to the 2017 EPA NEI and AP-42 (Belova et al., 2022). SO_2 from HO combustion is also coemitted with HCHO according to AP-42, our 6-factor PMF, and our sample of the house furnace exhaust. SO_2 from HO combustion can react with NH_3 and HCHO emitted by other combustion sources. The ADEC local profiles have 17 times more Fe for HO $PM_{2.5}$ than for, for example, RWC $PM_{2.5}$ (Ward, 2013), but NH_3 counteracts the impact of transition metals and encourages HMS formation via its impact on pH. In general, the secondary pathways are sensitive to aerosol water content, pH, temperature effects on pH and solubility etc., and are the subject of numerous other published and ongoing ALPACA studies (Campbell et al., 2022, 2024; Dingilian et al., 2024; Mao et al., 2024; Moon et al., 2024).

One study that quantified the relative importance of many of these pathways using isotopic analyses and IC for sulfur species on 12–24 hr filter samples collected at CTC concluded that the total IC particulate SO_4 during ALPACA was 62 ± 12% primary and 38 ± 12% secondary or 69 ± 15% primary and 31 ± 15% secondary for SO_4 in the $PM_{0.7}$ (Moon et al., 2024). If we assume all the non-SO_4 $PM_{0.7}$ sulfur (e.g., HMS and other S(IV) compounds) is also secondary, then the $PM_{0.7}$ sulfur is 59.5 ± 12.6% primary and 40.5 ± 12.6% secondary. In our 6-factor PMF solution, the AMS SO_4 was 85% primary, which is higher than the most comparable 69% measured for IC SO_4 on the filters. Assigning the 9-factor PMF factor number 6 as primary HO emissions implies the that AMS sulfate is ∼91% primary, while assigning factor number 6 as secondary PM implies the AMS sulfate is ∼45% primary. Since S(IV) compounds can be detected as sulfate using AMS, it is relevant that the lower PMF estimate of primary sulfate (45%) obtained by assuming factor 6 is all secondary aerosol is closer to the primary fraction of $PM_{0.7}$ total sulfur by the isotopic composition (59%) (Moon et al., 2024).

However, assigning factor 6 as secondary also implies that the campaign-average OA is 48% secondary, which we cannot confirm with other ALPACA measurements. Further, this assignment implies incorrectly that there are no BC or HCHO emissions from HO combustion; therefore, factor 6 may be mainly aged, but with some contribution from primary HO emissions that is not resolved by the PMF model. Some uncertainty in separating primary and secondary gases, PM, or AMS species may be expected when the model input does not have real-time data for a suite of unambiguously secondary species (e.g., real-time HMS). Also, the total period being investigated includes extremely low temperature episodes prone to interference with the AMS SO_4 and both January when the

Table 2
Key Features and PM Source Apportionment of Illustrative PMF Runs

Input data set	# of factors, 1 hr res.	BB-PM %	HO-PM%	Traffic-PM%	Aged-PM%
#1 Entire	6	20 (15–27)	41 (37–47)	28 (25–32)	9 (6–12)
#2 Entire	7	13	54	24	8
#2—Warm event	9 (F6 as HO)	13 (8–19)	57 (48–67)	28 (16–42)	1 (0–3)
#2—Warm event	9 (F6 as SA)	13 (8–19)	12 (8–17)	28 (16–42)	45 (39–54)
#2 Entire	10	9	32	35	24
#3 Entire	7	13	40	32	14
~Study-avg range	6–10	10–30	30–60	25–40	10–20+ (see text)

Note. If a single percentage is shown, it is the best estimate. The ranges for the PM source apportionment shown here and in the abstract and conclusions cover most of the spread in the PMF results from these and additional model runs based on "reasonable" input data.

AMS sulfate diel cycle suggests low amounts of secondary sulfate and February when the diel cycle has a noticeable afternoon peak suggesting significantly more secondary sulfate (Figure S6 in Supporting Information S1). Given the complexity, the simultaneous aging impacts on other PM components, and the difficulty of defining primary versus secondary, we do not expect PMF to precisely resolve primary and secondary PM or precisely quantify the contribution of each combustion source to the secondary growth. It is likely that SO_2 from HO combustion is a major PM precursor and both our 6- and 9-factor PMF solutions identified HO combustion as the second largest source of aromatic SOA precursors (after traffic). AP-42, our furnace sample, and our 6-factor PMF all identified HO combustion as significant sources of HCHO and acetaldehyde, which, along with SO_2, are potentially precursors for significant amounts of particulate S(IV) compounds (Mao et al., 2024). Future studies, including those based on PMF, might better define and distinguish primary and secondary PM and trace gases in general with more time-resolved measurements of unambiguously secondary species or increased consideration of the seasonal, daily, or even minute to minute time dependence of ambient conditions and source chemistry (Akagi et al., 2012; Bhandari et al., 2022; Dai et al., 2020; Mao et al., 2024; Yokelson et al., 2009). In terms of our original main motivation for embarking on these additional model runs, it is most important that neither assignment for factor 6 affects the BB contributions to $PM_{1.0}$ and CO, which are just 13 (8–19)% and 8 (3–16)%, respectively.

We ran the model with data set #2 and 10 factors to see if the aged and fresh sulfate would be partitioned differently. This resulted in 3 traffic factors, 2 aged factors, 2 HO factors, 2 BB factors, and the O_3 factor. The residuals were smaller and $PM_{1.0}$ was partitioned as traffic (35%), HO (32%), aged (24%), and BB (9%). Thus, there was some "migration" of PM to the HO factors from the aged factors. However, there were also mixed results in the strength of the factor assignments. For example, the HO factor contributions to the fit for each sample peaked very strongly during the cold event, but the agreement between the PMF HO profile and the local ADEC HO profile decreased ($r^2 = 0.69$). CO was attributed to traffic (57%), HO (20%), aged (11%), O_3-regional background (7%), and BB (5%). Model runs with 11 and 15 factors produced excellent fits, but some of the influential factors were more readily associated with individual species rather than complex, real-world sources. We ran the model with data set #3 at 1-min, 20-min, 1-hr, 2-hr, 3-hr, and 6-hr time resolution and 6–8 factors. At 2- to 6-hr time resolution, sources were not separated well. Finer time resolution consistently gave similar results for BB-PM and BB-CO (12%–13% and 0%–2%, respectively Table 2).

In summary, no substantial differences in the PMF runs were observed when using the different data sets, indicating that this analysis is quite resilient against reasonable changes made to the input data. Furthermore, the extensive PMF analyses conducted in this study and independent data from the VOC and aethalometer measurements at the house and AMS measurements at CTC suggest that the PM at the house site in Fairbanks is not simply dominated by "fresh"/primary emissions from BB or HO. Rather, traffic and secondary sources should also be considered significant in the present and evolving Fairbanks airshed. This does not suggest that existing or potential future RWC restrictions are misguided but highlights that reducing other sources could be beneficial in Fairbanks, particularly given the recent lowering of the annual $PM_{2.5}$ standard by both the USEPA and the World

Health Organization. In formulating mitigation strategies, many issues are important such as the population-weighted relevance of the measurement location, the benefits of compliance with EPA standards, fuel costs for residents etc.

4. Conclusions

First, we clarify that North Pole, which relies more on RWC than our study location, is the one location in the Fairbanks area that is out of compliance with the $PM_{2.5}$ standard, but it accounts for a small fraction of the Fairbanks metro area population. The ALPACA study was not conducted in North Pole to ascertain the most effective way to bring the whole Fairbanks area into compliance. Rather, ALPACA was designed to better understand both outdoor and indoor atmospheric chemistry in cold dark environments with a focus on Arctic, urban, wintertime chemistry where inversions can occur due to intense surface cooling in addition to topographical influences. This study, one of many under the ALPACA umbrella, focuses on the budget of trace gases and particles outdoors in a typical Fairbanks neighborhood using primarily concentrations, concentration ratios between species, correlations, diel cycles, and PMF. While contributions from woodsmoke may be lower in the neighborhood we sampled, the spatial variability in Fairbanks is such that, during strong surface-based inversions, local sources may have disproportionate implications for other sites (i.e., Hurst Road regulatory site) within the FNSB (Robinson et al., 2023). Therefore, we urge others to be cautious in using these results to assess attainment for the entire FNSB.

Adding together the mixing ratios of all the VOCs we measured in Fairbanks resulted in a median or average total VOC loading that was ∼50% to 4.5 times greater than that observed in winter in New York City or Boulder, CO likely due partly to the shallow surface layer. Aromatic VOCs accounted for ∼50% of the total measured VOCs in Fairbanks but only 5%–10% in NYC and Boulder. In contrast, ethanol was a smaller fraction of the total in Fairbanks than in the other locations and our PMF did not clearly identify contributions from volatile consumer products. We note that small gas-phase alkanes are likely important in Fairbanks, but they were not measured during ALPACA (or in the NYC and Boulder studies cited). We confirmed that the significant local evolution of the trace gases and particles can occur despite the short daylength. The local evolution can be spurred in part by the transport to Fairbanks of regional background air containing O_3, reaction of the "imported" O_3 with accumulated NO_2 to form the NO_3 radical, nonnegligible concentrations of OH and many other processes such as adduct formation in aerosol water and probably coagulation.

Thus, despite cold, dark conditions, and low oxidation ratios for SO_2 and NO_x, secondary processes made important contributions to the local burden of pollutants. Indeed, our comprehensive PMF analyses suggested that ∼10–20% of PM in Fairbanks during ALPACA could be due to aging. Specifically, in the 6-factor PMF solution, the aged factor accounted for ∼9% of SO_4, OA, and TNRM. The aged factor also accounted for 66% of NO_2 and 21% of HCHO. The 9-factor PMF solution added a factor that suggested the aging contributions could be higher for SO_4 and $PM_{1.0}$, but the factor likely combined contributions from both aging and primary HO combustion emissions that were not completely resolved.

Despite the importance of this aging and the cold temperatures favoring partitioning to the condensed phase, the majority of the reactive organic carbon is exported from Fairbanks in the gas phase and the fate of this reactive carbon on longer timescales warrants further investigation in future work. The remainder of the outdoor budget for particles and most trace gases is traceable to the combustion of fossil fuels and firewood. The contribution of the main combustion sources to total primary PM at the house site likely falls within these ranges: heating oil combustion (30%–60%), traffic (25%–40%), and RWC (10%–30%).

While this neighborhood studied does meet the EPA $PM_{2.5}$ standard, it may represent conditions for a significant fraction of the Fairbanks metro area population, and we observed days-long episodes of elevated $PM_{2.5}$ with peaks near 100 μg m^{-3} during ALPACA. Thus, improving air quality at the site is a worthwhile goal and justifies the recent lowering of the allowable sulfur content in heating oil. Our source apportionment taken together with earlier studies confirms a trend of increasing relative importance of traffic, secondary aerosol, and heating oil combustion along with decreasing relative importance of residential wood combustion in the Fairbanks PM budget. This is analogous to the general trend of organic emissions in US urban areas that as technology evolves

and the impact of past mitigation strategies matures, new targets for improving public health emerge (McDonald et al., 2018).

Data Availability Statement

Final data from the study is available to the scientific community at Arcticdata.io, which provides a portal to archival repositories of the field study's data (https://doi.org/10.18739/A2K35MG5H) (Ketcherside et al., 2025). The R project containing the compiled data and scripts designed to replicate analyses (aside from PMF) and generate figures can be retrieved from Zenodo at https://doi.org/10.5281/zenodo.15610198 (Ketcherside, 2025).

Acknowledgments
We thank the entire ALPACA science team of researchers for designing the experiment, acquiring funding, making measurements, and ongoing analysis of the results. The ALPACA project is organized as a part of the International Global Atmospheric Chemistry (IGAC) project under the Air Pollution in the Arctic: Climate, Environment and Societies (PACES) initiative with support from the International Arctic Science Committee (IASC), the National Science Foundation (NSF), and the National Oceanic and Atmospheric Administration (NOAA). We thank the University of Alaska Fairbanks and the Geophysical Institute for logistical support, and we thank Fairbanks for welcoming and engaging with this research. We would also like to thank Ryan Hoskins-Chaddon, who collected the O_3 measurements at the Birch Hill site. Purchase and preparation of the NO_x and O_3 instruments were supported by NSF Grant AGS-1349976 to R.Y. This study was supported by NOAA Climate Program Office's Atmospheric Chemistry, Carbon Cycle, and Climate program, Grant NA20OAR4310296 to UM. UM was additionally supported by the National Science Foundation (AGS # 2144896; EPSCoR # 2242802). P.F.D. and E.S.R. acknowledge funding support from NSF award NNA-2012905. W.R.S., J.M., and M.C.-M acknowledge support from NSF Grant NNA-1927750. W.R.S. and M.C.-M. also acknowledge support from NSF Grant AGS-2109134. J.M. also acknowledges support from NSF Grant AGS-2029747. K.A.P., A.L.H., and J.W. acknowledge support from NSF Grants RISE-1927831 and AGS-2037091. B.D. A., A.I., and B.T.-M. acknowledge support from the Agence National de Recherche (ANR) CASPA (Climate-relevant Aerosol Sources and Processes in the Arctic) project (Grant ANR-21-CE01-0017), Kathy Law (PI of the CASPA project), and the Institut polaire français Paul-Émile Victor (IPEV) (Grant 1215) and CNRS-INSU program LEFE (Les Enveloppes Fluides et l'Environnement) ALPACA-France projects. S.D. acknowledges support from the PRA (Programma di Ricerche in Artico) 2019 program (project A-PAW) and from the ENI-CNR Research Center Aldo Pontremoli. J. Stutz and J.K. acknowledge funding support from NSF Grants NNA-1927936 and AGS-2109240. B.A. and A.M. acknowledge funding support from NOAA Grant NA20OAR4310295.

References

Akagi, S. K., Craven, J. S., Taylor, J. W., McMeeking, G. R., Yokelson, R. J., Burling, I. R., et al. (2012). Evolution of trace gases and particles emitted by a chaparral fire in California. *Atmospheric Chemistry and Physics*, *12*(3), 1397–1421. https://doi.org/10.5194/acp-12-1397-2012

Akagi, S. K., Yokelson, R. J., Wiedinmyer, C., Alvarado, M. J., Reid, J. S., Karl, T., et al. (2011). Emission factors for open and domestic biomass burning for use in atmospheric models. *Atmospheric Chemistry and Physics*, *11*(9), 4039–4072. https://doi.org/10.5194/acp-11-4039-2011

Belova, A., Dagli, R., Economu, N., Hartley, S., Holder, C., Hubbard, H., et al. (2022). Literature review on the impacts of residential combustion - Final report. Retrieved from https://www.lung.org/policy-advocacy/healthy-air-campaign/healthy-efficient-homes/residential-combustion

Bhandari, S., Arub, Z., Habib, G., Apte, J. S., & Hildebrandt Ruiz, L. (2022). Source apportionment resolved by time of day for improved deconvolution of primary source contributions to air pollution. *Atmospheric Measurement Techniques*, *15*(20), 6051–6074. https://doi.org/10.5194/amt-15-6051-2022

Brett, N., Law, K. S., Arnold, S. R., Fochesatto, J. G., Raut, J.-C., Onishi, T., et al. (2025). Investigating processes influencing simulation of local Arctic wintertime anthropogenic pollution in Fairbanks, Alaska, during ALPACA-2022. *Atmospheric Chemistry and Physics*, *25*(2), 1063–1104. https://doi.org/10.5194/acp-25-1063-2025

Burkholder, J. B., Sander, S. P., Abbatt, J. P. D., Barker, J. R., Cappa, C., Crounse, J. D., et al. (2020). *Chemical kinetics and photochemical data for use in atmospheric studies; evaluation number 19*. Jet Propulsion Laboratory, National Aeronautics and Space Administration. Retrieved from https://hdl.handle.net/2014/49199

Busby, B. D., Ward, T. J., Turner, J. R., & Palmer, C. P. (2016). Comparison and evaluation of methods to apportion ambient PM2.5 to residential wood heating in Fairbanks, AK. *Aerosol and Air Quality Research*, *16*(3), 492–503. https://doi.org/10.4209/aaqr.2015.04.0235

Campbell, J. R., Battaglia, M., Dingilian, K., Cesler-Maloney, M., St Clair, J. M., Hanisco, T. F., et al. (2022). Source and chemistry of hydroxymethanesulfonate (HMS) in Fairbanks, Alaska. *Environmental Science & Technology*, *56*(12), 7657–7667. https://doi.org/10.1021/acs.est.2c00410

Campbell, J. R., Battaglia, M., Jr., Dingilian, K. K., Cesler-Maloney, M., Simpson, W. R., Robinson, E. S., et al. (2024). Enhanced aqueous formation and neutralization of fine atmospheric particles driven by extreme cold. *Science Advances*, *10*(36), eado4373. https://doi.org/10.1126/sciadv.ado4373

Carrico, C. M., Prenni, A. J., Kreidenweis, S. M., Levin, E. J. T., McCluskey, C. S., DeMott, P. J., et al. (2016). Rapidly evolving ultrafine and fine mode biomass smoke physical properties: Comparing laboratory and field results. *Journal of Geophysical Research: Atmospheres*, *121*(10), 5750–5768. https://doi.org/10.1002/2015JD024389

Coggon, M. M., Stockwell, C. E., Claflin, M. S., Pfannerstill, E. Y., Xu, L., Gilman, J. B., et al. (2024). Identifying and correcting interferences to PTR-ToF-MS measurements of isoprene and other urban volatile organic compounds. *Atmospheric Measurement Techniques*, *17*(2), 801–825. https://doi.org/10.5194/amt-17-801-2024

Coggon, M. M., Veres, P. R., Yuan, B., Koss, A., Warneke, C., Gilman, J. B., et al. (2016). Emissions of nitrogen-containing organic compounds from the burning of herbaceous and arboraceous biomass: Fuel composition dependence and the variability of commonly used nitrile tracers. *Geophysical Research Letters*, *43*(18), 9903–9912. https://doi.org/10.1002/2016GL070562

Dai, Q., Bi, X., Song, W., Li, T., Liu, B., Ding, J., et al. (2019). Residential coal combustion as a source of primary sulfate in Xi'an, China. *Atmospheric Environment*, *196*, 66–76. https://doi.org/10.1016/j.atmosenv.2018.10.002

Dai, Q., Liu, B., Bi, X., Wu, J., Liang, D., Zhang, Y., et al. (2020). Dispersion normalized PMF provides insights into the significant changes in source contributions to PM 2.5 after the COVID-19 outbreak. *Environmental Science & Technology*, *54*(16), 9917–9927. https://doi.org/10.1021/acs.est.0c02776

Decker, Z. C. J., Robinson, M. A., Barsanti, K. C., Bourgeois, I., Coggon, M. M., DiGangi, J. P., et al. (2021). Nighttime and daytime dark oxidation chemistry in wildfire plumes: An observation and model analysis of FIREX-AQ aircraft data. *Atmospheric Chemistry and Physics*, *21*(21), 16293–16317. https://doi.org/10.5194/acp-21-16293-2021

Dingilian, K., Hebert, E., Battaglia, M., Campbell, J. R., Cesler-Maloney, M., Simpson, W., et al. (2024). Hydroxymethanesulfonate and sulfur (IV) in fairbanks winter during the ALPACA study. *ACS ES&T Air*, *1*(7), 646–659. https://doi.org/10.1021/acsestair.4c00012

Edwards, K. C., Kapur, S., Fang, T., Cesler-Maloney, M., Yang, Y., Holen, A. L., et al. (2024). Residential wood burning and vehicle emissions as major sources of environmentally persistent free radicals in Fairbanks, Alaska. *Environmental Science & Technology*, *58*(32), 14293–14305. https://doi.org/10.1021/acs.est.4c01206

Fachinger, F., Drewnick, F., Gieré, R., & Borrmann, S. (2017). How the user can influence particulate emissions from residential wood and pellet stoves: Emission factors for different fuels and burning conditions. *Atmospheric Environment*, *158*, 216–226. https://doi.org/10.1016/j.atmosenv.2017.03.027

Finlayson-Pitts, B. J., & Pitts, J. N., Jr. (2000). *Chemistry of the upper and lower atmosphere: Theory, experiments, and applications* (1st ed.). Academic Press.

Gilman, J. B., Lerner, B. M., Kuster, W. C., Goldan, P. D., Warneke, C., Veres, P. R., et al. (2015). Biomass burning emissions and potential air quality impacts of volatile organic compounds and other trace gases from fuels common in the US. *Atmospheric Chemistry and Physics*, *15*(24), 13915–13938. https://doi.org/10.5194/acp-15-13915-2015

Gkatzelis, G. I., Coggon, M. M., McDonald, B. C., Peischl, J., Gilman, J. B., Aikin, K. C., et al. (2021). Observations confirm that volatile chemical products are a major source of petrochemical emissions in U.S. cities. *Environmental Science & Technology*, *55*(8), 4332–4343. https://doi.org/10.1021/acs.est.0c05471

Gkatzelis, G. I., Coggon, M. M., Stockwell, C. E., Hornbrook, R. S., Allen, H., Apel, E. C., et al. (2024). Parameterizations of US wildfire and prescribed fire emission ratios and emission factors based on FIREX-AQ aircraft measurements. *Atmospheric Chemistry and Physics*, *24*(2), 929–956. https://doi.org/10.5194/acp-24-929-2024

Heald, C. L., Goldstein, A. H., Allan, J. D., Aiken, A. C., Apel, E., Atlas, E. L., et al. (2008). Total observed organic carbon (TOOC) in the atmosphere: A synthesis of North American observations. *Atmospheric Chemistry and Physics*, *8*(7), 2007–2025. https://doi.org/10.5194/acp-8-2007-2008

Heald, C. L., Gouw, J. D., Goldstein, A. H., Guenther, A. B., Hayes, P. L., Hu, W., et al. (2020). Contrasting reactive organic carbon observations in the southeast United States (SOAS) and Southern California (CalNex). *Environmental Science & Technology*, *54*(23), 14923–14935. https://doi.org/10.1021/acs.est.0c05027

Hobbs, P. V., Sinha, P., Yokelson, R. J., Christian, T. J., Blake, D. R., Gao, S., et al. (2003). Evolution of gases and particles from a savanna fire in South Africa. *Journal of Geophysical Research*, *108*(D13), 8485. https://doi.org/10.1029/2002JD002352

Hu, L., Millet, D. B., Baasandorj, M., Griffis, T. J., Turner, P., Helmig, D., et al. (2015). Isoprene emissions and impacts over an ecological transition region in the U.S. upper midwest inferred from tall tower measurements. *Journal of Geophysical Research: Atmospheres*, *120*(8), 3553–3571. https://doi.org/10.1002/2014JD022732

Huangfu, Y., Yuan, B., Wang, S., Wu, C., He, X., Qi, J., et al. (2021). Revisiting acetonitrile as tracer of biomass burning in anthropogenic-influenced environments. *Geophysical Research Letters*, *48*(11), e2020GL092322. https://doi.org/10.1029/2020GL092322

Ijaz, A., Temime-Roussel, B., Chazeau, B., Albertin, S., Arnold, S. R., Barrett, B., et al. (2024). Complementary aerosol mass spectrometry elucidates sources of wintertime sub-micron particle pollution in Fairbanks, Alaska, during ALPACA 2022. *EGUsphere*, *2024*, 1–33. https://doi.org/10.5194/egusphere-2024-3789

Jaffe, D. A., Schnieder, B., & Inouye, D. (2022). Technical note: Use of PM2.5 to CO ratio as an indicator of wildfire smoke in urban areas. *Atmospheric Chemistry and Physics*, *22*(18), 12695–12704. https://doi.org/10.5194/acp-22-12695-2022

Juncosa Calahorrano, J. F., Lindaas, J., O'Dell, K., Palm, B. B., Peng, Q., Flocke, F., et al. (2021). Daytime oxidized reactive nitrogen partitioning in western U.S. wildfire smoke plumes. *Journal of Geophysical Research: Atmospheres*, *126*(4), e2020JD033484. https://doi.org/10.1029/2020JD033484

Ketcherside, D. (2025). *dtketcherside/ALPACA-house-outdoor-source-apportionment: v2.0.0 (v.2.0.0) [Collection]*. Zenodo. https://doi.org/10.5281/zenodo.15610198

Ketcherside, D., Hu, L., Yokelson, R., & Selimovic, V. (2025). Indoor and outdoor trace gas measurements at the house site in Fairbanks, Alaska during the Alaskan Layered Pollution And Chemical Analysis (ALPACA) 2022 field study [Dataset]. *NSF Arctic Data Center*. https://doi.org/10.18739/A2K35MG5H

Kotchenruther, R. A. (2016). Source apportionment of PM2.5 at multiple northwest U.S. sites: Assessing regional winter wood smoke impacts from residential wood combustion. *Atmospheric Environment*, *142*, 210–219. https://doi.org/10.1016/j.atmosenv.2016.07.048

Liu, X., Huey, L. G., Yokelson, R. J., Selimovic, V., Simpson, I. J., Müller, M., et al. (2017). Airborne measurements of western U.S. wildfire emissions: Comparison with prescribed burning and air quality implications. *Journal of Geophysical Research: Atmospheres*, *122*(11), 6108–6129. https://doi.org/10.1002/2016JD026315

Mao, J., Bali, K., Campbell, J. R., Robinson, E. S., DeCarlo, P. F., Ijaz, A., et al. (2024). Multiphase sulfur chemistry facilitates particle growth in a cold and dark urban environment. *Faraday Discussions*, *258*, 357–374. https://doi.org/10.1039/D4FD00170B

Marques, B., Kostenidou, E., Valiente, A. M., Vansevenant, B., Sarica, T., Fine, L., et al. (2022). Detailed speciation of non-methane volatile organic compounds in exhaust emissions from diesel and gasoline euro 5 vehicles using online and offline measurements. *Toxics*, *10*(4), 184. https://doi.org/10.3390/toxics10040184

May, A. A., Levin, E. J. T., Hennigan, C. J., Riipinen, I., Lee, T., Collett, J. L., et al. (2013). Gas-particle partitioning of primary organic aerosol emissions: 3. Biomass burning. *Journal of Geophysical Research: Atmospheres*, *118*(19), 11327–11338. https://doi.org/10.1002/jgrd.50828

McClure, C. D., & Jaffe, D. A. (2018). Investigation of high ozone events due to wildfire smoke in an urban area. *Atmospheric Environment*, *194*, 146–157. https://doi.org/10.1016/j.atmosenv.2018.09.021

McDonald, B. C., de Gouw, J. A., Gilman, J. B., Jathar, S. H., Akherati, A., Cappa, C. D., et al. (2018). Volatile chemical products emerging as largest petrochemical source of urban organic emissions. *Science*, *359*(6377), 760–764. https://doi.org/10.1126/science.aaq0524

Moon, A., Jongebloed, U., Dingilian, K. K., Schauer, A. J., Chan, Y.-C., Cesler-Maloney, M., et al. (2024). Primary sulfate is the dominant source of particulate sulfate during winter in Fairbanks, Alaska. *ACS ES&T Air*, *1*(3), 139–149. https://doi.org/10.1021/acsestair.3c00023

Müller, M., Anderson, B. E., Beyersdorf, A. J., Crawford, J. H., Diskin, G. S., Eichler, P., et al. (2016). In situ measurements and modeling of reactive trace gases in a small biomass burning plume. *Atmospheric Chemistry and Physics*, *16*(6), 3813–3824. https://doi.org/10.5194/acp-16-3813-2016

Norris, G. A., Duvall, R., Brown, S., & Bai, S. (2014). *EPA positive matrix factorization (PMF) 5.0 fundamentals and user guide (5.0)* (pp. 1–136). U.S. Environmental Protection Agency Office of Research and Development. Retrieved from https://www.epa.gov/sites/default/files/2015-02/documents/pmf_5.0_user_guide.pdf

Office of Research and Development. (1978). In *Workshop proceedings on primary sulfate emissions from combustion sources - Volume 2: Combustion sources*. US Environmental Protection Agency. (EPA 600-9-78-020b). Retrieved from https://nepis.epa.gov/Exe/ZyPURL.cgi?Dockey=9101C7RB.txt%0A

Office of Transportation and Air Quality. (2016). *Heavy-duty highway compression-ignition engines and urban buses: Exhaust emission standards*. U.S. Environmental Protection Agency Office of Transportation and Air Quality. Retrieved from https://www.epa.gov/emission-standards-reference-guide/epa-emission-standards-heavy-duty-highway-engines-and-vehicles

Paatero, P., Eberly, S., Brown, S. G., & Norris, G. A. (2014). Methods for estimating uncertainty in factor analytic solutions. *Atmospheric Measurement Techniques*, *7*(3), 781–797. https://doi.org/10.5194/amt-7-781-2014

Pagonis, D., Selimovic, V., Campuzano-Jost, P., Guo, H., Day, D. A., Schueneman, M. K., et al. (2023). Impact of biomass burning organic aerosol volatility on smoke concentrations downwind of fires. *Environmental Science & Technology*, *57*(44), 17011–17021. https://doi.org/10.1021/acs.est.3c05017

Permar, W., Wang, Q., Selimovic, V., Wielgasz, C., Yokelson, R. J., Hornbrook, R. S., et al. (2021). Emissions of trace organic gases from western U.S. wildfires based on WE-CAN aircraft measurements. *Journal of Geophysical Research: Atmospheres*, *126*(11), e2020JD033838. https://doi.org/10.1029/2020JD033838

Permar, W., Wielgasz, C., Jin, L., Chen, X., Coggon, M. M., Garofalo, L. A., et al. (2023). Assessing formic and acetic acid emissions and chemistry in western U.S. wildfire smoke: Implications for atmospheric modeling. *Environmental Sciences: Atmospheres*, *3*(11), 1620–1641. https://doi.org/10.1039/D3EA00098B

Polissar, A. V., Hopke, P. K., Paatero, P., Malm, W. C., & Sisler, J. F. (1998). Atmospheric aerosol over Alaska: 2. Elemental composition and sources. *Journal of Geophysical Research*, *103*(D15), 19045–19057. https://doi.org/10.1029/98JD01212

Roberts, J. M., Stockwell, C. E., Yokelson, R. J., de Gouw, J., Liu, Y., Selimovic, V., et al. (2020). The nitrogen budget of laboratory-simulated western US wildfires during the FIREX 2016 Fire Lab study. *Atmospheric Chemistry and Physics*, *20*(14), 8807–8826. https://doi.org/10.5194/acp-20-8807-2020

Robinson, E. S., Battaglia, M., Jr., Campbell, J. R., Cesler-Maloney, M., Simpson, W., Mao, J., et al. (2024). Multi-year, high-time resolution aerosol chemical composition and mass measurements from Fairbanks, Alaska. *Environmental Sciences: Atmospheres*, *4*(6), 685–698. https://doi.org/10.1039/D4EA00008K

Robinson, E. S., Cesler-Maloney, M., Tan, X., Mao, J., Simpson, W., & DeCarlo, P. F. (2023). Wintertime spatial patterns of particulate matter in Fairbanks, AK during ALPACA 2022. *Environmental Sciences: Atmospheres*, *3*(3), 568–580. https://doi.org/10.1039/D2EA00140C

Sekimoto, K., Coggon, M. M., Gkatzelis, G. I., Stockwell, C. E., Peischl, J., Soja, A. J., & Warneke, C. (2023). Fuel-type independent parameterization of volatile organic compound emissions from Western US wildfires. *Environmental Science & Technology*, *57*(35), 13193–13204. https://doi.org/10.1021/acs.est.3c00537

Sekimoto, K., Koss, A. R., Gilman, J. B., Selimovic, V., Coggon, M. M., Zarzana, K. J., et al. (2018). High- and low-temperature pyrolysis profiles describe volatile organic compound emissions from western US wildfire fuels. *Atmospheric Chemistry and Physics*, *18*(13), 9263–9281. https://doi.org/10.5194/acp-18-9263-2018

Sekimoto, K., Li, S.-M., Yuan, B., Koss, A., Coggon, M., Warneke, C., & de Gouw, J. (2017). Calculation of the sensitivity of proton-transfer-reaction mass spectrometry (PTR-MS) for organic trace gases using molecular properties. *International Journal of Mass Spectrometry*, *421*, 71–94. https://doi.org/10.1016/j.ijms.2017.04.006

Selimovic, V., Yokelson, R. J., McMeeking, G. R., & Coefield, S. (2020). Aerosol mass and optical properties, smoke influence on O_3, and high NO_3 production rates in a western U.S. city impacted by wildfires. *Journal of Geophysical Research: Atmospheres*, *125*(16), e2020JD032791. https://doi.org/10.1029/2020JD032791

Selimovic, V., Yokelson, R. J., Warneke, C., Roberts, J. M., de Gouw, J., Reardon, J., & Griffith, D. W. T. (2018). Aerosol optical properties and trace gas emissions by PAX and OP-FTIR for laboratory-simulated western US wildfires during FIREX. *Atmospheric Chemistry and Physics*, *18*(4), 2929–2948. https://doi.org/10.5194/acp-18-2929-2018

Simpson, W. R., Mao, J., Cesler-Maloney, M., Davey, R., & Campbell, J. (2020). *SOX particulate precursor study Ft*. Wainwright Army Base, Alaska.

Simpson, W. R., Mao, J., Fochesatto, G. J., Law, K. S., DeCarlo, P. F., Schmale, J., et al. (2024). Overview of the Alaskan Layered Pollution and Chemical Analysis (ALPACA) field experiment. *ACS ES&T Air*, *1*(3), 200–222. https://doi.org/10.1021/acsestair.3c00076

Traviss, N., Allen, G., & Ahmadi, M. (2024). Criteria, greenhouse gas, and hazardous air pollutant emissions factors from residential cordwood and pellet stoves using an integrated duty cycle test protocol. *ACS ES\&T Air*, *1*(9), 1190–1202. https://doi.org/10.1021/acsestair.4c00135

Wang, Y., & Hopke, P. K. (2014). Is Alaska truly the great escape from air pollution? - Long term source apportionment of fine particulate matter in Fairbanks, Alaska. *Aerosol and Air Quality Research*, *14*(7), 1875–1882. https://doi.org/10.4209/aaqr.2014.03.0047

Wang, Y., Hopke, P. K., Rattigan, O. V., Chalupa, D. C., & Utell, M. J. (2012). Multiple-year black carbon measurements and source apportionment using Delta-C in Rochester, New York. *Journal of the Air & Waste Management Association*, *62*(8), 880–887. https://doi.org/10.1080/10962247.2012.671792

Wang, Y., Hopke, P. K., Rattigan, O. V., Xia, X., Chalupa, D. C., & Utell, M. J. (2011). Characterization of residential wood combustion particles using the two-wavelength aethalometer. *Environmental Science & Technology*, *45*(17), 7387–7393. https://doi.org/10.1021/es2013984

Ward, T. J. (2013). The fairbanks, Alaska PM2.5 source apportionment research study winters 2005/2006-2012/2013, and summer 2012. Final Report, Amendments 6 and 7. Retrieved from https://dec.alaska.gov/media/7083/fairbanks-cmb-report-univ-mt-final-122313.pdf

Wu, S., Alaimo, C. P., Zhao, Y., Green, P. G., Young, T. M., Liu, S., et al. (2024). O_3 sensitivity to NO_x and VOC during RECAP-CA: Implication for emissions control strategies. *ACS ES&T Air*, *1*(6), 536–546. https://doi.org/10.1021/acsestair.4c00026

Yang, Y., Battaglia, M. A., Mohan, M. K., Robinson, E. S., DeCarlo, P. F., Edwards, K. C., et al. (2024). Assessing the oxidative potential of outdoor PM 2.5 in wintertime Fairbanks, Alaska. *ACS ES&T Air*, *1*(3), 175–187. https://doi.org/10.1021/acsestair.3c00066

Ye, L., & Wang, Y. (2020). Long-term air quality study in Fairbanks, Alaska: Air pollutant temporal variations, correlations, and PM2.5 source apportionment. *Atmosphere*, *11*(11), 1203. https://doi.org/10.3390/atmos11111203

Yokelson, R. J., Christian, T. J., Bertschi, I. T., & Hao, W. M. (2003). Evaluation of adsorption effects on measurements of ammonia, acetic acid, and methanol. *Journal of Geophysical Research*, *108*(D20), 4649. https://doi.org/10.1029/2003JD003549

Yokelson, R. J., Crounse, J. D., DeCarlo, P. F., Karl, T., Urbanski, S., Atlas, E., et al. (2009). Emissions from biomass burning in the Yucatan. *Atmospheric Chemistry and Physics*, *9*(15), 5785–5812. https://doi.org/10.5194/acp-9-5785-2009

Yokelson, R. J., Griffith, D. W. T., & Ward, D. E. (1996). Open-path Fourier transform infrared studies of large-scale laboratory biomass fires. *Journal of Geophysical Research*, *101*(D15), 21067–21080. https://doi.org/10.1029/96JD01800

Zhang, Z., Zhang, Y., Wang, X., Lü, S., Huang, Z., Huang, X., et al. (2016). Spatiotemporal patterns and source implications of aromatic hydrocarbons at six rural sites across China's developed coastal regions. *Journal of Geophysical Research: Atmospheres*, *121*(11), 6669–6687. https://doi.org/10.1002/2016JD025115